


HOMOGENIZED LATTICE BOLTZMANN METHODS FOR FLUID FLOW THROUGH POROUS MEDIA – PART I: KINETIC MODEL DERIVATION

STEPHAN SIMONIS^{1,*}, NICOLAS HAFEN², JULIUS JESSBERGER³, DAVIDE DAPELO⁴,
GUDRUN THÄTER¹ AND MATHIAS J. KRAUSE³

Abstract. In this series of studies, we establish homogenized lattice Boltzmann methods (HLBM) for simulating fluid flow through porous media. Our contributions in part I are twofold. First, we assemble the targeted partial differential equation system by formally unifying the governing equations for non-stationary fluid flow in porous media. A matrix of regularly arranged, equally sized obstacles is placed into the fluid domain to model fluid flow through porous structures governed by the incompressible nonstationary Navier–Stokes equations (NSE). Depending on the ratio of geometric parameters in the solid matrix arrangement, several homogenized equations are obtained. We review existing methods for homogenizing the nonstationary NSE for specific porosities and discuss the applicability of the resulting model equations. Consequently, the homogenized NSE are expressed as targeted partial differential equations that jointly incorporate the derived aspects. Second, we propose a kinetic model, the homogenized Bhatnagar–Gross–Krook Boltzmann equation, which approximates the homogenized nonstationary NSE. We formally prove that the zeroth and first order moments of the kinetic model provide solutions to the mass and momentum balance variables of the macroscopic model up to specific orders in the scaling parameter. Based on the present contributions, in the sequel (part II), the homogenized NSE are consistently approximated by deriving a limit consistent HLBM discretization of the homogenized Bhatnagar–Gross–Krook Boltzmann equation.

Mathematics Subject Classification. 35Q30, 35Q20, 35B27.

Received December 4, 2023. Accepted January 20, 2025.

Keywords and phrases. Lattice Boltzmann methods, kinetic models, Navier–Stokes equations, porous media, nonstationary fluid flow, homogenization.

¹ Institute for Applied and Numerical Mathematics, Karlsruhe Institute of Technology, Karlsruhe, Germany.

² Institute of Mechanical Process Engineering and Mechanics, Karlsruhe Institute of Technology, Karlsruhe, Germany.

³ Lattice Boltzmann Research Group, Karlsruhe Institute of Technology, Karlsruhe, Germany.

⁴ Department of Civil and Environmental Engineering, University of Liverpool, Liverpool, UK.

*Corresponding author: stephan.simonis@kit.edu

LIST OF SYMBOLS

Expression	Meaning
NSE	Navier–Stokes equations
LBM	Lattice Boltzmann method
BGK	Bhatnagar–Gross–Krook
HNSE	Homogenized Navier–Stokes equations
HLBM	Homogenized lattice Boltzmann method
Ω	Domain of the porous media including solid and fluid regions
Ω_ϵ	Fluid void filling the porous media structure
$\partial\Omega$	Boundary of Ω
d	Dimension, $\Omega \in \mathbb{R}^d$
Y_i^ϵ	i th cell in porous structure
$Y_{S,i}^\epsilon, Y_{F,i}^\epsilon$	i th spherical obstacle where $1 \leq i \leq N(\epsilon)$; and i -th fluid void cell
$N(\epsilon)$	Number of solid obstacles in the porous structure
$H^1(X)$	Sobolev space $H^k(X) = W^{k,2}(X)$, where $k = 1$
$H_0^1(X)$	Functions $f \in H^1(X)$ with vanishing trace $f _{\partial X} = 0$
$H_{\text{div}}^1(X)$	Divergence-free functions $f \in H^1(X)$
$H_{\#}^1(X)$	X -periodic functions in $H^1(X)$
ϵ	Side length of geometric porous media cell containing one obstacle
a_ϵ	Size or diameter of solid obstacle
a_ϵ^{crit}	Critical obstacle size
σ_ϵ	Ratio function of cell side length and obstacle size
$\mathbf{u}_\epsilon, p_\epsilon$	Fluid velocity and pressure on cell scale (nonhomogenized)
$\tilde{\mathbf{u}}_\epsilon, \tilde{p}_\epsilon$	Extension of the solution $\mathbf{u}_\epsilon, p_\epsilon$
\mathbf{F}	Given force field
ν	Kinematic viscosity
C_i^ϵ	Control volume containing $Y_{S,i}^\epsilon$
\mathbf{M}	Porosity matrix
\mathbf{e}_k	k th unit basis vector of \mathbb{R}^d
ι_i^ϵ	Linear homeomorphism, mapping each cell to the unit cell
\mathbf{w}_k, q_k	Fluid velocity and pressure in k th stationary local model problem
\mathbf{A}	Permeability tensor
\mathbf{v}_k, p_k	Fluid velocity and pressure in k th stationary unit cell problem
Y	Unit cell
Y_S, Y_F	Solid part and fluid part of unit cell
Y_S^m	Model obstacle in the model problem
δ	Scaling prefactor for the case $a_\epsilon = \delta\epsilon$
\mathbf{n}	Outward pointing normal vector
\mathbf{w}^j, π^j	Fluid velocity and pressure in j th nonstationary unit cell problem
$\tilde{\mathbf{A}}(t)$	Time-dependent permeability tensor
C	Scaling constant for the cases $a_\epsilon = C\epsilon^n$, where $n \in \mathbb{N}$
σ	Constant limit value of ratio σ_ϵ in case of $a_\epsilon = \mathcal{O}(\epsilon^3)$
φ	Porosity
A	Eigenvalue of isotropic permeability tensor
f	Particle density function
\mathbf{c}_i	i th discrete velocity
$\tilde{\mathbf{c}}_i$	i th prefactored discrete velocity

1. INTRODUCTION

The governing equations for fluid flow in porous media typically consist of modified versions of the Navier–Stokes equations (NSE). Several mathematical models exist, depending on the type of application. Depending on the context of porous media flows, most models can be categorized as either mathematically motivated, or application-related.

For mathematical modeling of fluid flow through porous media, the incompressible NSE can be modified to include the effects of the solid matrix on the fluid flow in the void. Various different mathematical models exist (see [32, 48], and references therein). Here, we recall the rigorous construction of porous media flow models formulated in Allaire’s seminal works, see *e.g.* [1–8]. Therein, the geometric definition of porous media as sets of equidistant obstacles in the flow domains is considered to construct model equations *via* homogenization. As a result, several homogenization limits are derived, whereby the homogenized equations depend on the geometric configuration. We distinguish between three classical cases of homogenization limits:

- incompressible NSE,
- Brinkman law,
- Darcy’s law.

The respective limits in this categorization were rigorously proved for the stationary [7] and nonstationary Stokes regime [6], as well as for the stationary NSE [5] as starting points. Although suggested by Allaire, to the knowledge of the authors, the validity of the stationary categorization of homogenization limits is not completely proven for the nonstationary NSE. Nevertheless, the works of Mikelić [44, 45] and Feireisl *et al.* [20] cover the homogenization limit toward the Brinkman law and Darcy’s law in the non-stationary case in a different framework. Other contributions also used this structural categorization, see *e.g.* [26, 34, 42]. Although these models are likely to be interconnected, rigorous proofs of the underlying relations are rare and limited to linear and stationary settings. For instance, Allaire [2] proved the compliance of a formally derived Darcy’s law and the Darcy’s law derived *via* homogenization (low volume fraction limit). Feppon [21] and Feppon *et al.* [22] proved high-order homogenization limits for the Stokes equations in a unified procedure. To the knowledge of the authors, the latter is the first and only derivation covering all three classical cases together with the low volume fraction limit at once. However, it should be noted that these unified studies have not been conducted for homogenizing the nonstationary NSE, yet.

Besides the mathematically rigorous model derivation, application-based model construction has been found to be suitable for fluid flow in porous media [27, 49, 67]. Typically, empirical observations and matching terms are used to introduce model systems akin to Brinkman [13], Forchheimer [23], Darcy [17], or mixed-type equations [48]. Depending on the characteristic scales of porosity in the application in question, the heuristically derived models can correctly recover flow physics or are severely in disagreement with experiments [48]. However, due to the large variation of involved spatial scales, the model equations are often solved numerically with highly parallelizable methods. For example, Spaid and Phelan [67] proposed a lattice Boltzmann method (LBM) for approximating Stokes and Stokes–Brinkman equations as target models. The latter only apply to large obstacles in the porous matrix and solely recover stationary flows. The LBM meanwhile is an established numerical technique for the approximate solution of various transport problems. An extensive introduction to LBM can be found, for example, in the review by Lallemand *et al.* [41] and references therein. Conceptually, LBMs approximating macroscopic fluid flow models, such as the NSE, can be derived by discretizing mesoscopic Boltzmann-like equations with simplified collision operators. In this case, the discretization has to be derived such that the desired limit of moments of the particle distribution functions towards solutions of the macroscopic equations is preserved [28]. This can be ensured, for example, with a limit consistent discretization [56, 58]. The classical discretizations, leading *e.g.* to second order consistency in space and first order in time to the NSE, result in an explicit scheme that is based on a theoretically embarrassingly parallelizable evolution equation for the discrete particle distribution functions. Providing distinct advantages in terms of parallelizability, the LBM is well suited for computational fluid dynamics and multiphysics simulations where good scalability on high-performance computing (HPC) facilities is crucial [14, 16, 29, 30, 37, 46, 56, 57, 59–63, 65, 66, 69]. Even standard LBM

formulations offer an easy to implement and mostly second order accurate, intrinsically matrix-free algorithm in space-time. Those are well-suited for approximating nonstationary and nonlinear problems and, if optimized properly, also capable of saturating modern-day HPC machinery [38,39].

The kinetic model derived in the present work can potentially recover several homogenization limit regimes and thus stands out from previous models in the literature. For example, Padhy *et al.* [50] have proposed a graded multiscale topology optimization, where the underlying Darcy model, though also including an inverse permeability model, recovers low-Reynolds (stationary) incompressible (linear) Stokes flow only. Seta [55] proposed an LBM that approximates a two-dimensional Brinkman equation based on an additional forcing term. In contrast to that, we develop the model in three dimensions and modify the kinetic equilibrium function directly to account for a permeability term in the macroscopic limit. Tanabe *et al.* [68] developed a density-based topology optimization method for natural convection problems by extending the adjoint LBM proposed by Krause *et al.* [36] combined with a forcing term accounting for an initially homogenized fluid–solid domain. Although this model operates in two and three dimensions, the permeability terms are modeled by a force instead of extending the equilibrium function as in the present work.

To the knowledge of the authors, an LBM based on modified equilibrium functions has not yet been used to approximate the nonstationary homogenized NSE that governs time-dependent and nonlinear (possibly turbulent) fluid flow through abstracted porous media.

Consequently, the overall aim of this series of works is to construct homogenized LBMs (HLBMs) that approximate the governing equations for homogenized nonstationary nonlinear fluid flow through porous media.

Our contributions in part I are twofold. First, we assemble the targeted partial differential equation (PDE) system by formally unifying the governing equations for nonstationary fluid flow in homogenized porous media. To this end, a matrix of regularly arranged obstacles of equal size is placed in the fluid domain to model fluid flow through structures of different porosities governed by the incompressible nonstationary NSE. Depending on the ratio of geometric parameters in the matrix arrangement, several cases of homogenized PDEs are obtained. We review existing methods to homogenize the stationary NSE. From that we assemble a conjecture for the cases of PDE models resulting from homogenization of the nonstationary NSE for specific porosities. Moreover, we interpret connections between the resulting model equations from the perspective of applicability. Consequently, the homogenized nonstationary NSE are formulated as unified targeted PDE system which jointly incorporates the derived aspects. Second, we propose a kinetic model, named homogenized Bhatnagar–Gross–Krook (BGK) Boltzmann equation, which approximates the homogenized nonstationary NSE in a diffusive scaling limit. We formally prove that the zeroth and first order moments of the kinetic model provide solutions to the mass and momentum balance variables of the macroscopic model up to specific orders in the scaling parameter.

Based on the present contributions, in the sequel (part II [64]) the homogenized NSE are consistently approximated by deriving a HLBM discretization of the homogenized BGK Boltzmann equation (see Fig. 1). Therein, a top-down derivation of HLBMs is provided, based on the limit consistent discretizations [58] of Boltzmann-like equations with simplified collision. We thus construct homogenized lattice Boltzmann equations that are up to second order consistent toward the pressure and the velocity of the HNSE, respectively. As the present case is different from [58], but uses the same steps in the derivation of the lattice Boltzmann equation, we adopted the abbreviations and extended them where necessary. Thus, we sketch the complete procedure to arrive at the final homogenized lattice Boltzmann equation in Figure 1, although the present work (part I) considers only parts of it.

This work is structured as follows. In Section 2, we summarize the geometric setup and the mathematical model based on homogenization of the stationary and the nonstationary NSE. In addition, its physical interpretation is discussed. In Section 3, the homogenized BGK Boltzmann equation is constructed as kinetic model based on a porosity modified equilibrium. Convergence of the zeroth and first order moments towards variables which obey the mass and momentum balance equations of the HNSE is formally proven. Finally, in Section 4 we critically assess the present work, suggest follow-up studies, and conclude the manuscript.

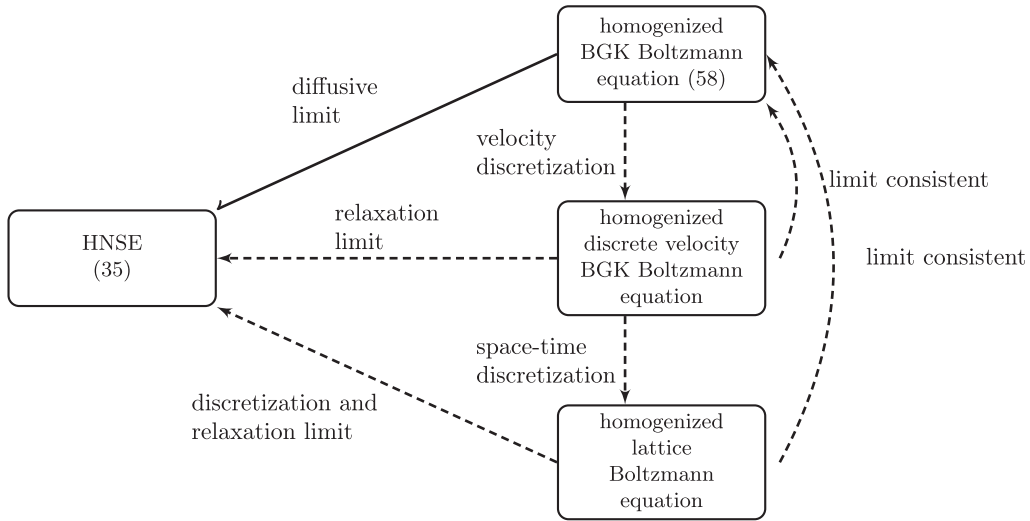


FIGURE 1. Limit consistent derivation of HLBM to approximate the HNSE (35). Limits considered in the present work are drawn with solid lines. Derivations considered in the sequel [64] are dashed.

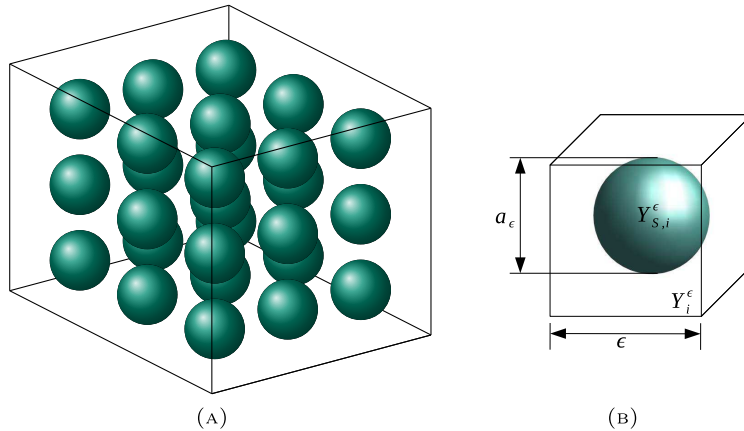


FIGURE 2. Illustrations of the geometric model of a porous structure in $d = 3$ dimensions. The i th cell is denoted with Y_i^ϵ containing a spherical matrix obstacle $Y_{S,i}^\epsilon$ with radius a_ϵ . Each cell is cubic with side length ϵ . (a) Subvolume of the porous media. (b) The i th cell.

2. MATHEMATICAL MODEL

2.1. Geometric setup

Unless stated otherwise, $C, C_n > 0$ are constants, where $n \in \mathbb{N}_0$. We model geometrically the flow through porous media *via* placing regularly arranged obstacles of equal size in the fluid domain [1, 3, 5, 8]. Let the domain $\Omega \subseteq \mathbb{R}^d$, $d \geq 2$ be defined as an open, bounded, and connected set. The boundary $\partial\Omega$ is assumed to be smooth of class C^1 . The domain Ω is covered with a regular mesh of period $\epsilon > 0$ (see Fig. 2a), prescribing the cells

$Y_i^\epsilon = (0, \epsilon)^d$, for $1 \leq i \leq N(\epsilon)$ (see Fig. 2b), where

$$N(\epsilon) = |\Omega|\epsilon^{-d}(1 + \mathcal{O}(1)) \tag{1}$$

counts their number. Each cubical cell contains a solid spherical obstacle $Y_{S,i}^\epsilon$ of diameter a_ϵ located in its center and a complementary part filled with fluid

$$Y_{F,i}^\epsilon = Y_i^\epsilon \setminus Y_{S,i}^\epsilon. \tag{2}$$

The overall fluid void is thus obtained *via* removal of the collective solid matrix, *i.e.*

$$\Omega_\epsilon = \Omega \setminus \bigcup_{i=1}^{N(\epsilon)} Y_{S,i}^\epsilon. \tag{3}$$

Further, we assume that all obstacles are similar to a model obstacle Y_S^m of size a_ϵ .

Under the assumption that the obstacle diameter is much smaller than the cell length, *i.e.* $a_\epsilon \ll \epsilon$ or equivalently

$$\lim_{\epsilon \searrow 0} \frac{a_\epsilon}{\epsilon} = 0, \tag{4}$$

we introduce a notion of respective size for the obstacle, by defining the ratio

$$\sigma_\epsilon = \begin{cases} \left(\frac{\epsilon^d}{a_\epsilon^{d-2}}\right)^{\frac{1}{2}} & \text{for } d \geq 3, \\ \epsilon |\log(\frac{a_\epsilon}{\epsilon})|^{\frac{1}{2}} & \text{for } d = 2. \end{cases} \tag{5}$$

Proposition 2.1. *For a critical size $a_\epsilon = a_\epsilon^{\text{crit}}$, defined as*

$$a_\epsilon^{\text{crit}} = \begin{cases} C_0 \epsilon^{\frac{d}{d-2}} & \text{for } d \geq 3, \\ e^{-\frac{C_0}{\epsilon^2}} & \text{for } d = 2, \end{cases} \tag{6}$$

with $0 < C_0 < \infty$, the ratio σ_ϵ reaches the nonnegative constant homogenization limit

$$\lim_{\epsilon \searrow 0} \sigma_\epsilon = \begin{cases} (C_0)^{\frac{2-d}{2}} & \text{for } d \geq 3, \\ (C_0)^{\frac{1}{2}} & \text{for } d = 2. \end{cases} \tag{7}$$

Proof. Substituting (6) into (5) completes the proof. □

Below in Section 2.2, it will be shown that, for $\epsilon \searrow 0$, large obstacles correspond to the limit $\sigma_\epsilon \rightarrow \infty$, small obstacles to the limit $\sigma_\epsilon \rightarrow 0$, and critical obstacles to the limit σ_ϵ with $0 < \sigma < \infty$.

2.2. Homogenized stationary Navier–Stokes equations

In the case of independence from time, the incompressible fluid flow in Ω_ϵ is modeled by the stationary nonlinear NSE $_\epsilon$

$$\begin{cases} \mathbf{u}_\epsilon \cdot \nabla_{\mathbf{x}} \mathbf{u}_\epsilon - \nu \Delta_{\mathbf{x}} \mathbf{u}_\epsilon = \mathbf{F} - \nabla_{\mathbf{x}} p_\epsilon & \text{in } \Omega_\epsilon, \\ \operatorname{div}_{\mathbf{x}} \mathbf{u}_\epsilon = 0 & \text{in } \Omega_\epsilon, \\ \mathbf{u}_\epsilon = \mathbf{0} & \text{on } \partial\Omega_\epsilon, \end{cases} \tag{8}$$

where $\mathbf{u}_\epsilon: \Omega_\epsilon \rightarrow \mathbb{R}^d$ denotes the velocity field, $p_\epsilon: \Omega_\epsilon \rightarrow \mathbb{R}$ is the scalar-valued pressure, $\mathbf{F} \in L^2(\Omega)^d$ defines a given force, and $\nu > 0$ is a constant viscosity. Additionally, to comply with (3), we define the extension to Ω of a pair of solutions $(\mathbf{u}_\epsilon, p_\epsilon)$ of (8) as

$$(\tilde{\mathbf{u}}_\epsilon, \tilde{p}_\epsilon) = \begin{cases} (\mathbf{u}_\epsilon, p_\epsilon) & \text{in } \Omega_\epsilon, \\ \left(\mathbf{0}, \frac{1}{|C_i^\epsilon|} \int_{C_i^\epsilon} p_\epsilon \, d\mathbf{x} \right) & \text{in each obstacle } Y_{S,i}^\epsilon, \end{cases} \tag{9}$$

where C_i^ϵ denotes a control volume containing $Y_{S,i}^\epsilon$ [5]. Heuristically, this means setting inside the obstacle zero velocity and the average value of the pressure field in its immediate proximity.

Based on the above definitions, Allaire [5] (see Cor. 1.4 therein) proved homogenization limits for different obstacle sizes expressed in the ratio (5). The results of homogenizing (8) are summarized in the following statements which are recalled without proof. Let the index \cdot_0 of a function space denote the classical vanishing trace operator, e.g. for $X \subseteq \mathbb{R}^d$ let

$$H_0^1(X) = \{f \in H^1(X) \mid f|_{\partial X} = 0\}. \tag{10}$$

Theorem 2.2. *According to the scaling of the obstacle size, we distinguish between three homogenization limits.*

(i) *If the obstacles are too small, i.e. $\lim_{\epsilon \searrow 0} \sigma_\epsilon = +\infty$, then $(\tilde{\mathbf{u}}_\epsilon, \tilde{p}_\epsilon)$ converges strongly in $H_0^1(\Omega)^d \times L^2(\Omega)/\mathbb{R}$ to (\mathbf{u}, p) , a solution of the stationary nonlinear NSE*

$$\begin{cases} \mathbf{u} \cdot \nabla_{\mathbf{x}} \mathbf{u} - \nu \Delta_{\mathbf{x}} \mathbf{u} = \mathbf{F} - \nabla_{\mathbf{x}} p & \text{in } \Omega, \\ \operatorname{div}_{\mathbf{x}} \mathbf{u} = 0 & \text{in } \Omega, \\ \mathbf{u} = \mathbf{0} & \text{on } \partial\Omega. \end{cases} \tag{11}$$

(ii) *If the obstacles have a critical size, i.e. $\lim_{\epsilon \searrow 0} \sigma_\epsilon = \sigma > 0$, then $(\tilde{\mathbf{u}}_\epsilon, \tilde{p}_\epsilon)$ converges weakly in $H_0^1(\Omega)^d \times L^2(\Omega)/\mathbb{R}$ to (\mathbf{u}, p) , a solution of the stationary nonlinear Brinkman law*

$$\begin{cases} \mathbf{u} \cdot \nabla_{\mathbf{x}} \mathbf{u} - \nu \Delta_{\mathbf{x}} \mathbf{u} + \frac{\nu}{\sigma^2} \mathbf{M} \mathbf{u} = \mathbf{F} - \nabla_{\mathbf{x}} p & \text{in } \Omega, \\ \operatorname{div}_{\mathbf{x}} \mathbf{u} = 0 & \text{in } \Omega, \\ \mathbf{u} = \mathbf{0} & \text{on } \partial\Omega. \end{cases} \tag{12}$$

(iii) *If the obstacles are too big, i.e. $\lim_{\epsilon \searrow 0} \sigma_\epsilon = 0$, then the rescaled solution $\left(\frac{\tilde{\mathbf{u}}_\epsilon}{\sigma_\epsilon}, \tilde{p}_\epsilon\right)$ converges strongly in $H_{\operatorname{div}}^1(\Omega)^d \times L^2(\Omega)/\mathbb{R}$ to (\mathbf{u}, p) , the unique solution of the Darcy’s law*

$$\begin{cases} \mathbf{u} = \frac{1}{\nu} \mathbf{M}^{-1} (\mathbf{F} - \nabla_{\mathbf{x}} p) & \text{in } \Omega, \\ \operatorname{div}_{\mathbf{x}} \mathbf{u} = 0 & \text{in } \Omega, \\ \mathbf{u} \cdot \mathbf{n} = \mathbf{0} & \text{on } \partial\Omega, \end{cases} \tag{13}$$

where $\mathbf{n} \in \mathbb{R}^d$ is the outward pointing normal vector.

In the regimes (ii) and (iii), \mathbf{M} is the same $d \times d$ symmetric matrix which depends only on the model obstacle Y_S^m .

Proof. Proofs for all cases are provided in [5]. □

The porosity matrix \mathbf{M} , which inversely represents a permeability tensor (see below Thm. 2.6), is computable via a model problem defined locally around Y_S^m (see Prop. 1.2 in [5] and Prop. 1.3.2 in [8]). The following result, obtained from merging Proposition 1.2 in [5] and Proposition 1.3.2 in [8], unfolds the computation of \mathbf{M} .

Proposition 2.3. Let $\{e_k\}_{1 \leq k \leq d}$ denote the unit basis of \mathbb{R}^d . Hence, the local model problem is defined for each k as

$$\begin{cases} \nabla_{\mathbf{x}} q_k - \Delta_{\mathbf{x}} \mathbf{w}_k = 0 & \text{in } \mathbb{R}^d \setminus Y_S^m, \\ \operatorname{div}_{\mathbf{x}} \mathbf{w}_k = 0 & \text{in } \mathbb{R}^d \setminus Y_S^m, \\ \mathbf{w}_k = \mathbf{0} & \text{on } \partial Y_S^m, \\ \mathbf{w}_k \begin{cases} \rightarrow e_k & \text{for } d \geq 3 \\ \sim e_k \log(|\mathbf{x}|) & \text{for } d = 2 \end{cases} & \text{as } |\mathbf{x}| \nearrow \infty. \end{cases} \tag{14}$$

The matrix \mathbf{M} is then assembled through

$$\mathbf{M} = \begin{cases} \left[\int_{\mathbb{R}^d \setminus Y_S} \nabla_{\mathbf{x}} \mathbf{w}_k \cdot \nabla_{\mathbf{x}} \mathbf{w}_j \, d\mathbf{x} \right]_{1 \leq j, k \leq d} & \text{for } d \geq 3, \\ 4\pi \mathbf{I}_d & \text{for } d = 2. \end{cases} \tag{15}$$

Remark 2.4. Note that the standard derivation of the Darcy’s law uses the assumption that the obstacle size $a_\epsilon = \mathcal{O}(\epsilon)$. Presently, so far we have assumed a smaller obstacle size. Hence, the typical permeability tensor (often referred to as \mathbf{K}) is computed from a different model problem as the local model problem (14). Allaire [2] closely examines the relation of permeability tensors and porosity matrices, and states the following result.

Let the obstacle size be redefined as $a_\epsilon := \delta\epsilon = \mathcal{O}(\epsilon)$. Let ι_i^ϵ define a linear homeomorphism, mapping each cell to the unit cell $Y = (0, 1)^d$ and allocating solid and fluid parts therein, $Y_S = \iota_i^\epsilon(Y_{S,i}^\epsilon)$ and $Y_F = \iota_i^\epsilon(Y_{F,i}^\epsilon)$, respectively. Hence, the unit cell Y now is split into a fluid part $Y_F = Y \setminus Y_S$ and an obstacle Y_S which is of size $\delta > 0$ due to ι_i^ϵ resembling a rescaling with a homothety factor of ϵ^{-1} [45]. The following theorem states the outcome of the homogenization in this case.

Theorem 2.5. An extension $(\tilde{\mathbf{u}}_\epsilon, \tilde{p}_\epsilon)$ of the solution $(\mathbf{u}_\epsilon, p_\epsilon)$ of (8) exists, such that $\tilde{\mathbf{u}}_\epsilon$ converges weakly in $L^2(\Omega)^d$ to \mathbf{u} , and \tilde{p}_ϵ converges strongly in $L^{q'}(\Omega)/\mathbb{R}$ to p , for any $1 < q' < \beta$, where (\mathbf{u}, p) is the unique solution of the Darcy’s law

$$\begin{cases} \mathbf{u} = \frac{1}{\nu} \mathbf{A}(\mathbf{F} - \nabla_{\mathbf{x}} p) & \text{in } \Omega, \\ \operatorname{div}_{\mathbf{x}} \mathbf{u} = 0 & \text{in } \Omega, \\ \mathbf{u} \cdot \mathbf{n} = 0 & \text{on } \partial\Omega. \end{cases} \tag{16}$$

In the Darcy’s law (16), the porosity matrix \mathbf{A} is defined by

$$\mathbf{A} = \left[\int_{Y_F} \nabla_{\mathbf{x}} \mathbf{v}_k \cdot \nabla_{\mathbf{x}} \mathbf{v}_j \, d\mathbf{x} \right]_{1 \leq j, k \leq d}, \tag{17}$$

where for the canonical basis vector e_k , $1 \leq k \leq d$, of \mathbb{R}^d , \mathbf{v}_k is the unique solution in $H_{\#}^1(Y_F)^d$ of the unit cell problem

$$\begin{cases} \nabla_{\mathbf{x}} p_k - \Delta_{\mathbf{x}} \mathbf{v}_k = e_k & \text{in } Y_F, \\ \operatorname{div}_{\mathbf{x}} \mathbf{v}_k = 0 & \text{in } Y_F, \\ \mathbf{v}_k = \mathbf{0} & \text{on } \partial(Y_S), \end{cases} \tag{18}$$

where $H_{\#}^1(Y_F)$ denotes the Sobolev space of Y_F -periodic functions in $H^1(Y_F)$.

Proof. The theorem is a special case of Theorem 1.2.5 in [8] which restates the rigorous result of Mikelić [44]. Hence, we choose the specific constants in Theorem 1.2.5 from [8] as $\gamma = 4$ and $\beta > 1$ which completes the proof. \square

Further, the continuity in the low volume fraction limit ($\delta \searrow 0$) is verified through the following theorem, which links the permeability tensor \mathbf{A} (17) in the Darcy’s law (16) to the porosity matrix \mathbf{M} (15) in the Darcy’s law (13).

Theorem 2.6. *Let (p_k, \mathbf{v}_k) be the unique solution of the unit cell problem. Rescaling it, for $\mathbf{x} \in \delta^{-1}(Y \setminus Y_S)$, we can define*

$$\mathbf{v}_k^\delta(\mathbf{x}) = \delta^{d-2} \mathbf{v}_k(\delta \mathbf{x}), \tag{19}$$

$$p_k^\delta(\mathbf{x}) = \delta^{d-1} p_k(\delta \mathbf{x}). \tag{20}$$

Further, let (q_i, \mathbf{w}_i) be the unique solution of the local model problem. Then $(p_k^\delta, \mathbf{v}_k^\delta)$ converges weakly to

$$\sum_{i=1}^d (\mathbf{e}_i^T \mathbf{M}^{-1} \mathbf{e}_k)(q_i, \mathbf{w}_i) \tag{21}$$

in $[L^2_{\text{loc}}(\mathbb{R}^d \setminus Y_S)/\mathbb{R}] \times [H^1_{\text{loc}}(\mathbb{R}^d \setminus Y_S)]^d$. Additionally, the low volume fraction limit for the permeability tensor is given as

$$\begin{cases} \lim_{\delta \searrow 0} \delta^{d-2} \mathbf{A}(\delta) = \mathbf{M}^{-1}, & \text{for } d \geq 3, \\ \lim_{\delta \searrow 0} \frac{1}{|\log \delta|} \mathbf{A}(\delta) = \mathbf{M}^{-1}, & \text{for } d = 2. \end{cases} \tag{22}$$

Proof. The theorem is proven by Allaire [2] (see Thm. 3.1 therein). □

Remark 2.7. Thus, for the complete range $a_\epsilon \leq \mathcal{O}(\epsilon)$, the homogenized stationary equations (11), (12), (13) and (16) are obtained as limits of (8) and (9). Specifically, the case $a_\epsilon < \mathcal{O}(\epsilon)$ is covered in Theorem 2.2 via (i–iii), and the complementary case (iv) $a_\epsilon = \mathcal{O}(\epsilon)$, via Theorem 2.6.

2.3. Homogenized nonstationary Navier–Stokes equations

Let the domain be defined as above and $d \in \{2, 3\}$. The incompressible fluid flow, now being dependent on time $t \in I = (0, T)$, is governed by the nonstationary nonlinear NSE_ϵ

$$\begin{cases} \partial_t \mathbf{u}_\epsilon + \epsilon^4 \mathbf{u}_\epsilon \cdot \nabla_{\mathbf{x}} \mathbf{u}_\epsilon - \epsilon^2 \nu \Delta_{\mathbf{x}} \mathbf{u}_\epsilon = \mathbf{F} - \nabla_{\mathbf{x}} p_\epsilon & \text{in } \Omega_\epsilon \times I, \\ \operatorname{div}_{\mathbf{x}} \mathbf{u}_\epsilon = 0 & \text{in } \Omega_\epsilon \times I, \\ \mathbf{u}_\epsilon|_{t=0} = \mathbf{u}_{0,\epsilon} & \text{in } \Omega_\epsilon, \\ \mathbf{u}_\epsilon = \mathbf{0} & \text{on } \partial\Omega_\epsilon \times I, \end{cases} \tag{23}$$

where $\mathbf{u}_\epsilon : \Omega_\epsilon \times I \rightarrow \mathbb{R}^d$ denotes the velocity field, $p_\epsilon : \Omega_\epsilon \times I \rightarrow \mathbb{R}$ is the scalar-valued pressure, $\mathbf{F} \in L^2(I; L^2(\Omega_\epsilon)^d)$ defines a given force, $\nu > 0$ is a constant viscosity, and $\partial\Omega_\epsilon$ is supposed to be sufficiently regular.

Remark 2.8. Note that the individual terms of (23) are properly rescaled by prefactors of ϵ to ensure a non-vanishing limit velocity. In [8], it is stated that the very small viscosity balances the friction of the fluid on the obstacles’ boundaries. A more detailed explanation in terms of non-dimensional numbers is given in Section 1.1 of [45], where the ratio of squared characteristic length L_c and characteristic time T_c is assumed to scale as $\frac{L_c^2}{T_c} \sim \frac{1}{\nu \epsilon^2}$. In addition, it is assumed that $\frac{L_c}{V_c T_c} \sim \frac{1}{\epsilon^\beta}$, where V_c denotes the characteristic velocity, $\beta > 1$ in general and $\beta = 4$ in the present setting. These two assumption lead to the specific scaling in the nonstationary nonlinear NSE_ϵ (23) that we also adopt here. Interestingly, in [19] a different scaling, with a prefactor ϵ^2 in front of the time derivative only, leads to a porous medium equation when homogenizing the complete Navier–Stokes–Fourier system, which contrasts to the presently summarized results and indicates that the scaling of the pore-level equation plays a crucial role in the homogenization process.

Further, following [20], let

$$\begin{cases} \mathbf{u}_{0,\epsilon} \in L^2(\Omega_\epsilon)^d, \\ \operatorname{div}_{\mathbf{x}} \mathbf{u}_{0,\epsilon} = 0 & \text{in } \Omega_\epsilon, \\ \mathbf{u}_{0,\epsilon} \cdot \mathbf{n} = 0 & \text{on } \partial\Omega_\epsilon. \end{cases} \tag{24}$$

In this configuration, at least one weak solution to (23) exists [20], which is obtained in $\mathbf{u}_\epsilon \in L^2(I; H^1(\Omega_\epsilon)^d)$ and $p_\epsilon \in H^{-1}(I; L^2_0(\Omega_\epsilon))$, respectively [45]. To formulate the nonstationary version of Theorem 2.2, the works of Feireisl *et al.* [20], Allaire [6], and Mikelić [44] serve as a basis. Since only parts of the limit cases have been proven yet, we formulate a conjecture for the nonstationary case below.

Definition 2.9. Let

$$\begin{cases} \partial_t \mathbf{w}^j - \nu \Delta_{\mathbf{x}} \mathbf{w}^j + \nabla_{\mathbf{x}} \pi^j = \mathbf{0} & \text{in } Y_F \times I, \\ \operatorname{div}_{\mathbf{x}} \mathbf{w}^j = 0 & \text{in } Y_F \times I, \\ \mathbf{w}^j|_{t=0} = \mathbf{e}^j & \text{in } Y_F, \\ \mathbf{w}^j = \mathbf{0} & \text{on } (\partial Y_S \setminus \partial Y) \times I \end{cases} \quad (25)$$

define a time-dependent unit cell problem [45], where \mathbf{w}^j is $H^1(Y)$ -periodic and π^j is $L^2(Y)$ -periodic, component-wise. The matrix $\tilde{\mathbf{A}}(t)$ is then assembled through

$$\tilde{A}_{ij}(t) = \frac{1}{|Y|} \int_{Y_F} w_j^i(\mathbf{y}, t) \, d\mathbf{y}, \quad (26)$$

for $1 \leq i, j \leq d$.

Conjecture 2.10. Let $(\mathbf{u}_\epsilon, p_\epsilon)$ be a weak solution to (23). Assume that $\lim_{\epsilon \searrow 0} \mathbf{u}_{0,\epsilon} = \mathbf{u}_0$ weakly in $L^2(\Omega)^d$. According to the scaling regimes of the obstacle size, we distinguish between the following homogenization limits.

(i) If the obstacles are too small, *i.e.* $\lim_{\epsilon \searrow 0} \sigma_\epsilon = +\infty$, then $(\mathbf{u}_\epsilon, p_\epsilon)$ converges to (\mathbf{u}, p) , a solution of the nonstationary nonlinear NSE

$$\begin{cases} \partial_t \mathbf{u} + \mathbf{u} \cdot \nabla_{\mathbf{x}} \mathbf{u} - \nu \Delta_{\mathbf{x}} \mathbf{u} = \mathbf{F} - \nabla_{\mathbf{x}} p & \text{in } \Omega \times I, \\ \operatorname{div}_{\mathbf{x}} \mathbf{u} = 0 & \text{in } \Omega \times I, \\ \mathbf{u}|_{t=0} = \mathbf{u}_0 & \text{in } \Omega, \\ \mathbf{u} = \mathbf{0} & \text{on } \partial\Omega \times I. \end{cases} \quad (27)$$

(ii) If the obstacles have a critical size, *i.e.* $\lim_{\epsilon \searrow 0} \sigma_\epsilon = \sigma > 0$, then $(\mathbf{u}_\epsilon, p_\epsilon)$ converges in $L^2(\Omega \times I)$ and weakly in $L^2(I; W_0^{1,2}(\Omega))$ to (\mathbf{u}, p) , respectively, a solution of the nonstationary nonlinear Brinkman law

$$\begin{cases} \partial_t \mathbf{u} + \mathbf{u} \cdot \nabla_{\mathbf{x}} \mathbf{u} - \nu \Delta_{\mathbf{x}} \mathbf{u} + \frac{\nu}{\sigma^2} \mathbf{M} \mathbf{u} = \mathbf{F} - \nabla_{\mathbf{x}} p & \text{in } \Omega \times I, \\ \operatorname{div}_{\mathbf{x}} \mathbf{u} = 0 & \text{in } \Omega \times I, \\ \mathbf{u}|_{t=0} = \mathbf{u}_0 & \text{in } \Omega, \\ \mathbf{u} = \mathbf{0} & \text{on } \partial\Omega \times I. \end{cases} \quad (28)$$

(iii) If the obstacles are smaller than $\mathcal{O}(\epsilon)$, but exceed the critical size, such that $\lim_{\epsilon \searrow 0} \sigma_\epsilon = 0$, then a suitably rescaled version of $(\mathbf{u}_\epsilon, p_\epsilon)$ converges to (\mathbf{u}, p) , the unique solution of the time-dependent Darcy’s law

$$\begin{cases} \partial_t \mathbf{u} + \nu \mathbf{M} \mathbf{u} = \mathbf{F} - \nabla_{\mathbf{x}} p & \text{in } \Omega \times I, \\ \operatorname{div}_{\mathbf{x}} \mathbf{u} = 0 & \text{in } \Omega \times I, \\ \mathbf{u}|_{t=0} = \mathbf{u}_0 & \text{in } \Omega, \\ \mathbf{u} \cdot \mathbf{n} = \mathbf{0} & \text{on } \partial\Omega \times I. \end{cases} \quad (29)$$

(iv) If the obstacles are of size $\mathcal{O}(\epsilon)$, then the rescaled solution $(\epsilon^2 \mathbf{u}_\epsilon, \partial_t p_\epsilon)$ converges in $L^2(I; \Omega)^d$ and weakly in $H^{-1}(I; L^2_0(\Omega))$, respectively to (\mathbf{u}, p) , the unique solution of the Darcy’s law with memory

$$\begin{cases} \nu \mathbf{u} - \tilde{\mathbf{A}}(t) \mathbf{u}_0 = \int_0^t \tilde{\mathbf{A}}(t-s) [\mathbf{F}(s) - \nabla_{\mathbf{x}} p(s)] \, ds & \text{in } \Omega \times I, \\ \operatorname{div}_{\mathbf{x}} \mathbf{u} = 0 & \text{in } \Omega \times I, \\ \mathbf{u} \cdot \mathbf{n} = \mathbf{0} & \text{on } \partial\Omega \times I. \end{cases} \quad (30)$$

Further, if the flow stabilizes after a finite period of time, the Darcy’s law with memory (30) contracts for $t \nearrow \infty$ to the classical Darcy’s law (16) with

$$A_{ij} = \int_0^\infty \tilde{A}_{ij}(t) dt, \tag{31}$$

for $1 \leq i, j, \leq d$.

In the regimes (i–iii), \mathbf{M} is the same $d \times d$ symmetric matrix as in Proposition 2.3 and depends only on the model obstacle Y_S^m . In case of (iv), $\tilde{\mathbf{A}}(t)$ is constructed from Definition 2.9.

Proof of cases (ii) and (iv). In contrast to the stationary case (see Thms. 2.2, 2.5 and 2.6) only parts of the homogenization limits in Conjecture 2.10 have been proven yet. In addition, to the knowledge of the authors, none of the interconnections between individual cases (i–iv) have been established yet. Hence, we recall the available proofs only. Feireisl *et al.* [20] proved case (ii), where obstacles of critical size smaller than $\mathcal{O}(\epsilon)$ are considered. However, a different methodology from the one used by Allaire is applied to rigorously pass to the limit equations. Using the techniques used in [20], the above assumptions on the shape and location of obstacles can be loosened. The resulting homogenized equations, however, are a Brinkman law which is similar to the one obtained in the framework introduced above. The case (iv) above is a special case of the derivations in Mikelić [45] (see Thm. 1.2 therein, with $\beta = 4$) and is thus rigorously proven. \square

Remark 2.11. Cases (i) and (iii) are based on the conclusive evidence in the literature (see *e.g.* [3, 20]) for the resulting PDEs when homogenizing the nonlinear nonstationary NSE (23). For a rigorous proof, starting from the homogenization limits of the nonstationary Stokes equations established in [6] could be promising, since, as stated in [3], the inclusion of a nonlinear advective term to the Stokes equations resembles a compact perturbation of the ϵ -dependent stationary nonlinear NSE (8). It is also notable that for case (iii), a proof for the homogenization of the nonstationary Stokes equations (without the nonlinear advective term) is given in [6]. Concerning the low volume fraction limit which connects cases (iv) to (iii), the memory effective terms of the Darcy’s law with memory (30) might induce the time-dependency in the time-dependent Darcy’s law (29). Hence, an import of stationary effects and an additional solving for time-dependent eigenvalue problems in respective cell spaces [2] might be insightful.

2.4. Applicability of the homogenized model

Assumption 2.12. To establish a connection to experimentally conforming model equations, we make the following assumptions:

- (1) According to [11, 45], the stabilization of the Darcy’s law with memory (30) toward the classical Darcy’s law (16) is understood to happen in a short period of time. Hence, we assume a stabilized flow in case of obstacle sizes which obey Conjecture 2.10 case (iv), *i.e.* the homogenization limit is constituted by an ordinary Darcy’s law. Similarly, we assume stabilization for case (iii). Typically this involves adding Brinkman terms (diffusion) or other necessary features to the Darcy’s law (30) in case (iv). Though these artificial features are effective in the void and within the porous–void interface, they are contracted to zero within the porous media under the necessary local assumptions of highly viscous and stabilized (stationary) flow.
- (2) The porosity, defined as $\varphi := |\Omega_\epsilon|/|\Omega|$, is assumed to be constant in Ω_T .
- (3) The medium is isotropic, which results in regular symmetric, hence diagonal or diagonalizable matrices \mathbf{M} and \mathbf{A} . Further, we may thus reduce the matrix \mathbf{A} or \mathbf{M}^{-1} to its only eigenvalue, which yields a scalar multiplication. Below we assume this simplification and unless stated otherwise, denote the single eigenvalue of \mathbf{A} with A .

Remark 2.13. Assumption 2.12 supports the commonly formulated Brinkman equation [32, 48], which is constituted by a classical Darcy’s law plus a diffusion term. Neglecting the time-dependency in the Brinkman law

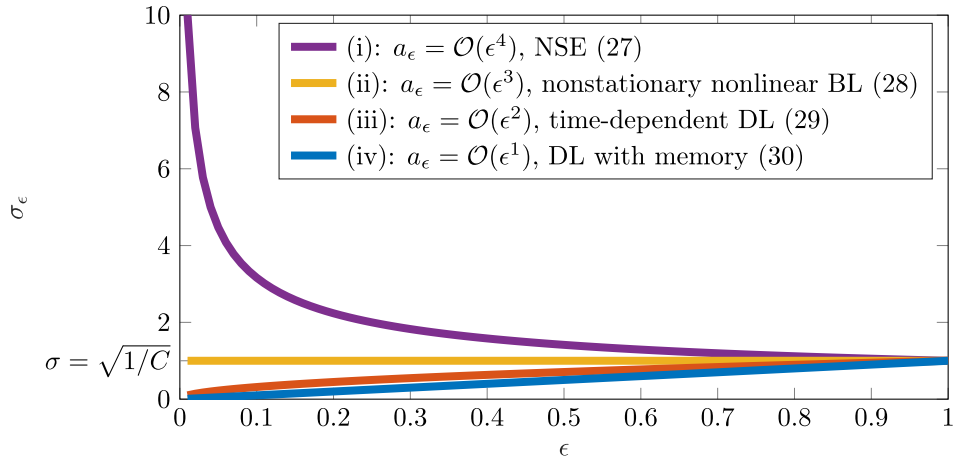


FIGURE 3. Graph of ratio $\sigma_\epsilon(\epsilon)$ (32) for $d = 3$ and $C = 1$.

derived above as well as its inertial terms, results in a simplified equation which solely respects diffusion. To match the porous–void interface, Spaid and Phelan [67] used such a Brinkman equation as a stationary limit for their simulations. A note in [67] additionally states that far from the interface, and within the porous domain region, the governing equation reduces again, to the classical Darcy’s law [67]. It should however be noted that along the stationary limit, the nonstationary solution to the method in [67] is rather a Brinkman law as presently formulated, which was not further examined therein.

For $d = 3$ (see Fig. 2b), σ_ϵ describes the square root of the ratio of the cell volume to the obstacle diameter

$$\sigma_\epsilon = \left(\frac{\epsilon^3}{a_\epsilon} \right)^{\frac{1}{2}}. \tag{32}$$

We use the classical notion of porosity [32] to assess the above framework in terms of applicability.

Proposition 2.14. *For Conjecture 2.10(iv) we obtain the minimal porosity of $\varphi \approx 0.4764$.*

Proof. We limit our analysis to polynomial ansatz up to degree 4. Recalling Conjecture 2.10, the size a_ϵ of the obstacles for $d = 3$ can be distinguished in the order of ϵ as follows. Let $0 < C < \epsilon$ be a constant prefactor.

- (i) Let $a_\epsilon = C\epsilon^4 = \mathcal{O}(\epsilon^4)$. Then $\sigma_\epsilon = \left(\frac{1}{C\epsilon}\right)^{\frac{1}{2}} \Rightarrow \lim_{\epsilon \searrow 0} \sigma_\epsilon = +\infty$.
- (ii) Let $a_\epsilon = C\epsilon^3 = \mathcal{O}(\epsilon^3)$. Then $\sigma_\epsilon = \left(\frac{1}{C}\right)^{\frac{1}{2}} \Rightarrow \lim_{\epsilon \searrow 0} \sigma_\epsilon = \sigma > 0$.
- (iii) Let $a_\epsilon = C\epsilon^2 = \mathcal{O}(\epsilon^2)$. Then $\sigma_\epsilon = \left(\frac{\epsilon}{C}\right)^{\frac{1}{2}} \Rightarrow \lim_{\epsilon \searrow 0} \sigma_\epsilon = 0$.
- (iv) Let $a_\epsilon = C\epsilon^1 = \mathcal{O}(\epsilon^1)$. Then $\sigma_\epsilon = \left(\frac{\epsilon^2}{C}\right)^{\frac{1}{2}} \Rightarrow \lim_{\epsilon \searrow 0} \sigma_\epsilon = 0$.

For the purpose of illustration, the limits of σ_ϵ for the cases (i–iv) are plotted in Figure 3 with a fixed constant $C = 1$. Subsequent to forming the porosity parameter φ as the ratio of void and full domain, the injection of

the magnitude approximation for a_ϵ yields

$$\varphi = \frac{|\Omega_\epsilon|}{|\Omega|} = \frac{\left| \Omega - \bigcup_{i=1}^{N(\epsilon)} Y_{S,i}^\epsilon \right|}{|\Omega|} = 1 - \frac{\left| \bigcup_{i=1}^{N(\epsilon)} Y_{S,i}^\epsilon \right|}{|\Omega|} = 1 - \frac{\pi a_\epsilon^3}{6\epsilon^3} = \begin{cases} 1 - \frac{C\pi}{6}\epsilon^9 & \text{in case (i),} \\ 1 - \frac{C\pi}{6}\epsilon^6 & \text{in case (ii),} \\ 1 - \frac{C\pi}{6}\epsilon^3 & \text{in case (iii),} \\ 1 - \frac{C\pi}{6} & \text{in case (iv)} \end{cases} \quad (33)$$

$$\xrightarrow{\epsilon \searrow 0} \begin{cases} 1 & \text{in cases (i–iii),} \\ 1 - \frac{C\pi}{6} & \text{in case (iv),} \end{cases} \quad (34)$$

where $|\cdot|$ denotes the Lebesgue measure of the standard Euclidean space. The claim follows from setting $C = 1$ in (34). \square

Remark 2.15. Proposition 2.14 frames the modeling possibilities of the presented approach, since the minimal attainable porosity is similar to a square sphere packing [24, 48]. The formal computations above thus imply physical reasoning for the theoretical homogenization limit equations in Conjecture 2.10. The fact that nonuniform porosity can only be reached in the limit equations of case (iv) has, to the knowledge of the authors, not been explicitly stated before.

Remark 2.16. A lower porosity could be obtained *e.g.* by considering flow through two-dimensional porous media in three dimensions, or by choosing three-dimensional obstacles in different arrangements [15, 48]. Whereas the former becomes reasonable when modeling for example fibers as obstacles with a circular cross-section [10] and repeating above calculations for $d = 2$, the latter renders rather complicated, due to the necessity of proving Conjecture 2.10 under loosened initial topological assumptions on the obstacles [20]. The question if all four cases would be retained under a differentiability-breaking change of shape or cell-crossing shifts in location, remains to be answered.

Remark 2.17. Under Assumption 2.12 we formulate a unified Brinkman law for case Conjecture 2.10(ii) below (Def. 2.18), which depends on σ and formally limits

- either to the nonstationary nonlinear NSE in case (i) for $\sigma \nearrow \infty$
- or (*via* rescaling the solution to $\tilde{\mathbf{u}}/\sigma^2$) to the stabilized Darcy’s law in case (iii) and (iv) for $\sigma \searrow 0$.

Further, since the continuity in the low volume fraction limit [2] implies that \mathbf{M}^{-1} is the limit of \mathbf{A} , we use \mathbf{A} in the modified Brinkman law and, due to Assumption 2.12(3), reduce it to its single eigenvalue A . In summary, the resulting model equation is assumed to be valid for all herein considered porosities and permeabilities. We additionally motivate the procedure of emulating all four regimes by recent observations that turbulence prevails for porosity values approaching unity in aligned arrays of spheres [53].

Definition 2.18. Based on Conjecture 2.10, Assumption 2.12, Proposition 2.14 and Remark 2.17, we construct a unified nonstationary nonlinear Brinkman law

$$\begin{cases} \partial_t \mathbf{u} + \mathbf{u} \cdot \nabla_{\mathbf{x}} \mathbf{u} - \nu \Delta_{\mathbf{x}} \mathbf{u} + \frac{\nu}{\sigma^2} A^{-1} \mathbf{u} = \mathbf{F} - \nabla_{\mathbf{x}} p & \text{in } \Omega \times I, \\ \operatorname{div}_{\mathbf{x}} \mathbf{u} = 0 & \text{in } \Omega \times I, \\ \mathbf{u}|_{t=0} = \mathbf{u}_0 & \text{in } \Omega, \\ \mathbf{u} = \mathbf{0} & \text{on } \partial\Omega \times I, \end{cases} \quad (35)$$

which is used as a target PDE system for the kinetic model derivation below in Section 3, and is to be approximated with LBMs in the sequel [64]. Due to the unified perspective, the PDE system (35) is now referred to as homogenized NSE (HNSE) (35).

3. KINETIC MODEL DERIVATION

The overall goal of this series of works is to derive consistently a homogenized lattice Boltzmann equation for approximating the HNSE (35), which then forms the centerpiece of the final LBM algorithm. Conforming to the discretization approach of LBM, we couple one or more scaling parameters (*e.g.* $\varepsilon > 0$) of a Boltzmann-like equation to an artificially injected grid parameter $h \in \mathbb{R}_{>0}$. Toward this aim, in the present work we construct this kinetic equation in nondiscretized form which approximates the HNSE (35) in a (continuous) diffusive limit. The aim of the sequel (part II [64]) is then, to discretize the kinetic model while retaining the kinetic limit (see Fig. 1). The discretization is thus required to be limit consistent in the sense of [56, 58]. Since we aim for formal convergence of the final LBM only, the notion of limit consistency requires formal convergence of the kinetic model as well which is proven below.

3.1. Preliminaries

Let $\Omega \subseteq \mathbb{R}^d$ with $d = 3$ be a volume of rarefied gas which comprises many interacting particles. *Via* equalizing the mass $m \in \mathbb{R}_{>0}$, we interpret the particles as point masses. The state of a one-particle system is assumed to depend on position $\mathbf{x} \in \Omega$ and velocity $\mathbf{v} \in \Xi$ at time $t \in I = [t_0, t_1] \subseteq \mathbb{R}$ with $T \geq t_1 > t_0 > 0$, where $\Omega \subseteq \mathbb{R}^d$ denotes the positional space, $\Xi = \mathbb{R}^d$ is the velocity space, $\mathfrak{P} := \Omega \times \Xi$ is the phase space, and the crossing $\mathfrak{R} := \Omega \times \Xi \times I$ defines the phase-time tuple.

Definition 3.1. The probability density function

$$f: \mathfrak{R} \rightarrow \mathbb{R}_{>0}, (\mathbf{x}, \mathbf{v}, t) \mapsto f(\mathbf{x}, \mathbf{v}, t) \quad (36)$$

for the particles' positions $\mathbf{x} \in \Omega$ and velocities $\mathbf{v} \in \Xi$ at time $t \in I$ defines the state of the dynamical system which is governed by the Boltzmann equation (BE)

$$\left(\partial_t + \mathbf{v} \cdot \nabla_{\mathbf{x}} + \frac{\mathbf{F}}{m} \cdot \nabla_{\mathbf{v}} \right) f = J(f, f) \quad \text{in } \mathfrak{R}, \quad (37)$$

where

$$f|_{t=0} = f_0 \quad \text{in } \mathfrak{P} \quad (38)$$

supplements a suitable initial condition. The operator

$$J(f, f) = \int_{\mathbb{R}^3} \int_{S^2} |\mathbf{v} - \mathbf{w}| [f(\mathbf{x}, \mathbf{v}', t) f(\mathbf{x}, \mathbf{w}', t) - f(\mathbf{x}, \mathbf{v}, t) f(\mathbf{x}, \mathbf{w}, t)] d\mathbf{N} d\mathbf{w} \quad (39)$$

models the collision, where $d\mathbf{N}$ is the normalized surface integral with the unit vector $\mathbf{N} \in S^2$ and $(\mathbf{v}', \mathbf{w}')^T = T_{\mathbf{N}}(\mathbf{v}, \mathbf{w})^T$ result from the transformation $T_{\mathbf{N}}$ that models hard sphere collision [9].

Definition 3.2. Let f be given in the sense of (36). Then, *via* prefactored integration over $\Xi = \mathbb{R}^d$, we define the moments

$$n_f: \begin{cases} \Omega \times I \rightarrow \mathbb{R}_{>0}, \\ (\mathbf{x}, t) \mapsto n_f(\mathbf{x}, t) := \int_{\mathbb{R}^d} f(\mathbf{x}, \mathbf{v}, t) d\mathbf{v}, \end{cases} \quad (40)$$

$$\rho_f: \begin{cases} \Omega \times I \rightarrow \mathbb{R}_{>0}, \\ (\mathbf{x}, t) \mapsto \rho_f(\mathbf{x}, t) := m n_f(\mathbf{x}, t), \end{cases} \quad (41)$$

$$\mathbf{u}_f: \begin{cases} \Omega \times I \rightarrow \mathbb{R}^d, \\ (\mathbf{x}, t) \mapsto \mathbf{u}_f(\mathbf{x}, t) := \frac{1}{n_f(\mathbf{x}, t)} \int_{\mathbb{R}^d} \mathbf{v} f(\mathbf{x}, \mathbf{v}, t) d\mathbf{v}, \end{cases} \quad (42)$$

$$\mathbf{P}_f: \begin{cases} \Omega \times I \rightarrow \mathbb{R}^{d \times d}, \\ (\mathbf{x}, t) \mapsto \mathbf{P}_f(\mathbf{x}, t) := m \int_{\mathbb{R}^d} [\mathbf{v} - \mathbf{u}_f(\mathbf{x}, t)] \otimes [\mathbf{v} - \mathbf{u}_f(\mathbf{x}, t)] f(\mathbf{x}, \mathbf{v}, t) d\mathbf{v}, \end{cases} \quad (43)$$

$$p_f: \begin{cases} \Omega \times I \rightarrow \mathbb{R}_{>0}, \\ (\mathbf{x}, t) \mapsto p_f(\mathbf{x}, t) := \frac{1}{d} \sum_{i=1}^d (\mathbf{P}_f)_{i,i}(\mathbf{x}, t), \end{cases} \quad (44)$$

respectively as particle density, mass density, velocity, stress tensor, and pressure. Here and below, the moments of f are indexed with \cdot_f .

Notably, the absolute temperature θ is determined implicitly by an ideal gas assumption

$$p_f = n_f R \theta, \quad (45)$$

where $R > 0$ is the universal gas constant. To a dedicated order of magnitude in characteristic scales, the above moments approximate the macroscopic quantities conserved by the incompressible NSE [25]. Equilibrium states f^{eq} , defined by

$$J(f^{\text{eq}}, f^{\text{eq}}) = 0 \quad \text{in } \mathfrak{X}, \quad (46)$$

exist [25]. Via the gas constant $R = k_B/m \in \mathbb{R}_{>0}$ (where $k_B \in \mathbb{R}_{>0}$ is the Boltzmann constant) and $\theta \in \mathbb{R}_{>0}$, n_f as well as \mathbf{u}_f , the equilibrium state is found to be of Maxwellian form

$$f^{\text{eq}}(\mathbf{x}, \mathbf{v}, t): \begin{cases} \mathfrak{X} \rightarrow \mathbb{R}, \\ (\mathbf{x}, \mathbf{v}, t) \mapsto \frac{n_f(\mathbf{x}, t)}{(2\pi R\theta)^{\frac{d}{2}}} \exp\left(-\frac{[\mathbf{v} - \mathbf{u}_f(\mathbf{x}, t)]^2}{2R\theta}\right). \end{cases} \quad (47)$$

Remark 3.3. We identify f^{eq}/n_f as d -dimensional normal distribution for $\mathbf{v} \in \mathbb{R}^d$ with expectation \mathbf{u}_f and covariance $R\theta \mathbf{I}_d$. In this regard, the arguments of f^{eq} regularly appear in terms of moments $f^{\text{eq}}(n_f, \mathbf{u}_f, \theta)$ (see e.g. [31, 33, 35, 40]).

Lemma 3.4. *The moments ρ_f , \mathbf{u}_f and p_f are conserved by collision.*

Proof. From f^{eq}/n_f being a density function, we find

$$\rho_{f^{\text{eq}}} \stackrel{(41)}{=} m \int_{\mathbb{R}^d} f^{\text{eq}}(\mathbf{x}, \mathbf{v}, t) d\mathbf{v} = mn_f = \rho_f, \quad (48)$$

$$\mathbf{u}_{f^{\text{eq}}} \stackrel{(42)}{=} \frac{1}{n_{f^{\text{eq}}}} \int_{\mathbb{R}^d} \mathbf{v} f^{\text{eq}}(\mathbf{x}, \mathbf{v}, t) d\mathbf{v} = \mathbf{u}_f. \quad (49)$$

The covariance matrix of f^{eq}/n_f for a perfect gas (45), verifies the conservation of pressure

$$\begin{aligned} p_{f^{\text{eq}}} &\stackrel{(44)}{=} \frac{1}{d} m \int_{\mathbb{R}^d} (\mathbf{v} - \mathbf{u}_{f^{\text{eq}}})^2 f^{\text{eq}}(\mathbf{x}, \mathbf{v}, t) d\mathbf{v} \\ &= \frac{1}{d} m \int_{\mathbb{R}^d} (\mathbf{v} - \mathbf{u}_f)^2 f^{\text{eq}}(\mathbf{x}, \mathbf{v}, t) d\mathbf{v} \\ &= \frac{1}{d} mn_f \sum_{i=1}^d R\theta \\ &= p_f. \end{aligned} \quad (50)$$

□

Definition 3.5. According to the Bhatnagar–Gross–Krook (BGK) model [12], we simplify the collision operator J in (37) to

$$Q(f) := -\frac{1}{\tau}(f - M_f^{\text{eq}}) \quad \text{in } \mathfrak{R}, \tag{51}$$

where $\tau > 0$ denotes the relaxation time between collisions, and $M_f^{\text{eq}} = f^{\text{eq}}(\mathbf{x}, \mathbf{v}, t)$ is a formal particular Maxwellian determined by n_f and \mathbf{u}_f .

Remark 3.6. The essential benefit of (51) is to maintain the conservation of the moments ρ_f and \mathbf{u}_f while drastically reducing the complexity of the operator J defined in (39). Whereas the former ensures that the kinetic model has a macroscopic interpretation in terms of moments, the latter is specifically important for the purpose of discretization. In fact, the conservation of both ρ_f and \mathbf{u}_f , respectively (48) and (49), is upheld, since $\ln(M_f^{\text{eq}})$ is a collision invariant of Q (cf. Thm. 1.5 in [35]), i.e. $\int_{\mathbb{R}^d} \ln(M_f^{\text{eq}})Q(f) \, d\mathbf{v} = 0$.

Definition 3.7. With Q from (51) implanted in (37), the BGK Boltzmann equation (BGKBE) reads

$$\underbrace{\left(\partial_t + \mathbf{v} \cdot \nabla_{\mathbf{x}} + \frac{\mathbf{F}}{m} \cdot \nabla_{\mathbf{v}} \right)}_{= \frac{D}{Dt}} f = Q(f) \quad \text{in } \mathfrak{R}, \tag{52}$$

where $D/(Dt)$ is referred to as material derivative, and $f(\cdot, \cdot, 0) = f_0$ sets a suitable initial condition. Here and below, the variable f is renamed to obey (52) instead of (37).

Remark 3.8. Mostly under strict assumptions, several existence and uniqueness results for solutions to (52) have been proven in the past. The global existence of solutions to the BGK Boltzmann equation (52) has been rigorously proven in [51]. Weighted L^∞ bounds and uniqueness have later been established on bounded domains [52] and in \mathbb{R}^d [47]. Moreover, the hydrodynamic scaling limits of moments ρ_f and \mathbf{u}_f toward Leray’s weak solutions of the incompressible NSE [43] have been rigorously proven by Saint-Raymond [54]. Below, we will refer to this type of scaling limit as diffusive instead, due to the presence of diffusion terms in the macroscopic limit.

3.2. Homogenized BGK Boltzmann collision

As common to classical derivations in LBMs, we start with the mesoscopic viewpoint to formally assess the continuum limit toward the macroscopic target equation. Apart from the procedure itself being classical, to the knowledge of the authors, the results below are novel. Let K denote the single eigenvalue of the permeability tensor \mathbf{A} according to the Definition 2.18. All other definitions follow the notation in [56, 58].

Definition 3.9. Based on (47), the homogenized Maxwellian for the BGK collision (51) is defined as

$$M_f^{\text{eq}} = f^{\text{eq}}(n_f, \varpi \mathbf{u}_f, T) \tag{53}$$

with an additional prefactor called porosity control

$$\varpi = 1 - \nu \tau K^{-1} \tag{54}$$

in the velocity argument. For $\varpi = 1$, the collision reduces to the classical BGK operator (51).

For any ρ_f, \mathbf{u}_f, T and ϖ we obtain the zeroth, first and second order balance laws

$$\rho_{M_f^{\text{eq}}} = m \int_{\mathbb{R}^d} M_f^{\text{eq}} \, d\mathbf{v} = m \int_{\mathbb{R}^d} f^{\text{eq}}(n_f, \varpi \mathbf{u}_f, T) \, d\mathbf{v} = \rho_f, \tag{55}$$

$$\mathbf{u}_{M_f^{\text{eq}}} = \frac{1}{n_{M_f^{\text{eq}}}} \int_{\mathbb{R}^d} \mathbf{v} M_f^{\text{eq}} d\mathbf{v} = \frac{1}{n_f} \int_{\mathbb{R}^d} \mathbf{v} f^{\text{eq}}(n_f, \varpi \mathbf{u}_f, T) d\mathbf{v} = \varpi \mathbf{u}_f, \quad (56)$$

$$p_{M_f^{\text{eq}}} = \frac{m}{d} \int_{\mathbb{R}^d} (\mathbf{v} - \mathbf{u}_{M_f^{\text{eq}}})^2 M_f^{\text{eq}} d\mathbf{v} = \frac{m}{d} \int_{\mathbb{R}^d} (\mathbf{v} - \varpi \mathbf{u}_f)^2 f^{\text{eq}}(n_f, \varpi \mathbf{u}_f, T) d\mathbf{v} = p_f, \quad (57)$$

respectively. Notably, the hydrodynamic first order moment of M_f^{eq} in (56) differs from that of f^{eq} due to the prefactored porosity control ϖ .

Definition 3.10. With the homogenized M_f^{eq} from (53) implanted in (51), the homogenized BGK Boltzmann equation reads

$$\frac{D}{Dt} f = Q(f) \quad \text{in } \mathfrak{X}. \quad (58)$$

Remark 3.11. In the present mesoscopic framework, the term homogenized refers to generalizing the BGK Boltzmann equation as a special case for $\varpi = 1$ (via $K \nearrow \infty$) to a broader validity where $\varpi \neq 1$. Below, we formally indicate that for $\varpi < 1$ the homogenized Maxwellian (53) leads to imposing a nonstandard hydrodynamic similarity of the homogenized BGK Boltzmann equation (58) to the HNSE (35) in the broadest sense of Hilbert's sixth problem. The artificial case of $\varpi > 1$ is neglected hereafter.

3.3. Homogenized diffusive limit

Analogously to the derivation in [58], we relate the homogenized BGK Boltzmann equation (58) to the HNSE (35) by diffusive limiting. To this end, we formally verify that the assumed to be well-defined moments in Definition 3.2 obey the balance equations of the HNSE (35). The derivation is done in three steps (see [58]). The first step consists of a moment integration of the BGK Boltzmann equation (52) up to the order of the macroscopic moments ρ_f and \mathbf{u}_f . Whereas the moments ρ , \mathbf{u} , and p are approximated moment integrals on f in the final LBM, and serve as conserved variables for the macroscopic fluid model, the pressure tensor from the moment integration has no macroscopic meaning yet (it has to be derived or imposed). The second step introduces an expansion that allows to derive the expression of the pressure tensor moment in terms of the macroscopically conserved moments up to a specific order in the expansion parameter. The third step then finally uses the expansion from Step 2 to compute this formulation of the pressure tensor that is needed to complete Step 1. Indeed the expression is nothing else but Newton's hypothesis, recovered up to order two in the expansion parameter.

3.3.1. Step 1: Mass conservation and momentum balance

Let f^* be a solution to the homogenized BGK Boltzmann equation (58). Multiplying (58) by m and integrating over the velocity space $\Xi = \mathbb{R}^d$ yields the solenoidal constraint in (35) after division by the constant ρ_{f^*} , where the force term vanishes when applying Corollary 5.2 from [35] with $g = 1$ and $\mathbf{a} = \mathbf{F}$ in the respective notation. To balance momentum, we integrate $m\mathbf{v} \times (58)$ over the $\Xi = \mathbb{R}^d$ and obtain in Ω_T that

$$\begin{aligned} \partial_t(\rho_{f^*} \mathbf{u}_{f^*}) + \nabla_{\mathbf{x}} \cdot \mathbf{P}_{f^*} + (\rho_{f^*} \mathbf{u}_{f^*} \cdot \nabla_{\mathbf{x}}) \mathbf{u}_{f^*} + \mathbf{F} &= -\frac{1}{\tau} (\rho_{f^*} \mathbf{u}_{f^*} - \varpi \rho_{f^*} \mathbf{u}_{f^*}) \\ &= -\nu K^{-1} \rho_{f^*} \mathbf{u}_{f^*}. \end{aligned} \quad (59)$$

Besides the homogenization term on the right hand side, the derivation of (59) closely follows the procedure in [56, 58]. In the end, via (59)/ ρ_{f^*} we recover a balance law of momentum in conservative form where the additional term $-\nu K^{-1} \mathbf{u}_{f^*}$ is induced by the homogenization controlled equilibrium and corresponds to $-(\nu/(\sigma^2)) \mathbf{A}^{-1} \mathbf{u}$ under the assumptions on the porous structure made above. Hence, with a suitably defined \mathbf{P}_{f^*} conforming to the assumptions of incompressible Newtonian flow, the HNSE (35) is reached in the diffusive limit. This incompressible limit regime of the homogenized BGK Boltzmann equation (58) arises from parameter alignment to diffusion terms. We thus extend the derivation given in [35, 58] for the classical BGK Boltzmann equation to the homogenized BGK Boltzmann equation (58).

3.3.2. Step 2: Incompressible limit

We recall the definitions and assignments made in [58], i.e. the incompressible limit regime of the BGK Boltzmann equation (52) is obtained via aligning parameters to the diffusion terms [35, 58]. Based on that, we perform the same assignments here to obtain the homogenized BGK Boltzmann equation (58) in the diffusive limit. Let l_f be the mean free path, \bar{c} the mean absolute thermal velocity, and $\nu > 0$ a kinematic viscosity. Assuming that a characteristic length L and a characteristic velocity U are given, we define the Knudsen number, the Mach number and the Reynolds number, respectively

$$Kn := \frac{l_f}{L}, \tag{60}$$

$$Ma := \frac{U}{\bar{c}_s}, \tag{61}$$

$$Re := \frac{UL}{\nu}. \tag{62}$$

These nondimensional numbers relate as

$$Re = \frac{l_f \bar{c}_s}{\nu} \frac{Ma}{Kn} = \sqrt{\frac{24}{\pi}} \frac{Ma}{Kn}, \tag{63}$$

via defining $\nu := \pi \bar{c} l_f / 8$ and the isothermal speed of sound $\bar{c}_s := \sqrt{3R\theta}$ (see also [54] and references therein).

Definition 3.12. To link the mesoscopic distributions with the macroscopic continuum we inversely substitute \bar{c}_s with an artificial parameter $\varepsilon \in \mathbb{R}_{>0}$ through

$$\bar{c}_s \leftarrow \frac{1}{\varepsilon}. \tag{64}$$

Here and below, the symbol \leftarrow denotes the assignment operator.

In the limit $\varepsilon \searrow 0$, the incompressible continuum is reached, since Kn and Ma tend to zero while Re remains constant [54]. Based on that, we assign

$$\bar{c} = \sqrt{\frac{8k_B\theta}{m\pi}} \leftarrow \sqrt{\frac{8}{3\pi}} \frac{1}{\varepsilon}, \tag{65}$$

$$l_f \leftarrow \sqrt{\frac{24}{\pi}} \nu \varepsilon \tag{66}$$

and (65) unfold the relaxation time

$$\tau = \frac{l_f}{\bar{c}} \leftarrow 3\nu\varepsilon^2. \tag{67}$$

Definition 3.13. We reassign the so called porosity controller

$$\varpi \leftarrow 1 - 3\nu^2\varepsilon^2 K^{-1} =: \varpi_\varepsilon, \tag{68}$$

where $\varepsilon > 0$ is a scaling parameter, and define the ε -parametrized homogenized BGK Boltzmann equation, similarly to the ε -parametrized BGK Boltzmann equation in [58], as

$$\frac{D}{Dt} f = -\frac{1}{3\nu\varepsilon^2} (f - M_f^{\text{eq}}) \quad \text{in } \mathfrak{R}, \tag{69}$$

where the homogenized Maxwellian distribution evaluated at $(n_f, \varpi_\varepsilon \mathbf{u}_f)$ now reads

$$M_f^{\text{eq}} = \frac{n_f \varepsilon^d}{\left(\frac{2}{3}\pi\right)^{\frac{d}{2}}} \exp\left(-\frac{3}{2}(\mathbf{v}\varepsilon - \varpi_\varepsilon \mathbf{u}_f \varepsilon)^2\right) \quad \text{in } \mathfrak{R}. \tag{70}$$

The ε -parametrized homogenized BGK Boltzmann equation (69) is accordingly transformed to

$$f = M_f^{\text{eq}} - 3\nu\varepsilon^2 \frac{D}{Dt} f \quad \text{in } \mathfrak{R}. \quad (71)$$

Repeating the material derivative through $(D/(Dt))$ (71) yields

$$\frac{D}{Dt} f = \frac{D}{Dt} M_f^{\text{eq}} - 3\nu\varepsilon^2 \left(\frac{D}{Dt} \right)^2 f \quad \text{in } \mathfrak{R}. \quad (72)$$

The expression (72) serves to substitute $(D/(Dt))f$ in (71) which gives

$$f = M_f^{\text{eq}} - 3\nu\varepsilon^2 \frac{D}{Dt} M_f^{\text{eq}} + \left(3\nu\varepsilon^2 \frac{D}{Dt} \right)^2 f \quad \text{in } \mathfrak{R}. \quad (73)$$

Repeating the above subsequently produces higher order terms and substitutions. The evolving family unfolds the power series

$$f = \sum_{i=0}^{\infty} \left(-3\nu\varepsilon^2 \frac{D}{Dt} \right)^i M_f^{\text{eq}} \quad \text{in } \mathfrak{R}. \quad (74)$$

Remark 3.14. As already noted in [58], we can derive an expansion expression for f as a power series that can be used to approximate the pressure tensor in the following step. Up to lower order, the expansion series can also be obtained *via* Maxwell iteration based on an initial Taylor expansion of the material derivative or by a classical Chapman–Enskog expansion. However, it is to be noted that the present derivation starts with repeated application of the material derivative which is, to the knowledge of the authors, not the case for the Maxwell iteration procedure.

3.3.3. Step 3: Newton's hypothesis

To complete the macroscopic limit the stress tensor \mathbf{P}_{f^*} in (59) has to be matched to (35), which for a solution f^* to the homogenized BGK Boltzmann equation (58) yields

$$\mathbf{P}_{f^*} = -p_{f^*} \mathbf{I} + 2\nu\rho \mathbf{D}_{f^*} + \mathcal{O}(\varepsilon^b) \quad \text{in } \Omega_T \quad (75)$$

up to an order $b > 0$. Using (74), an approximation ansatz of the form

$$f^* = M_{f^*}^{\text{eq}} - 3\nu\varepsilon^2 \frac{D}{Dt} M_{f^*}^{\text{eq}} \quad \text{in } \mathfrak{R} \quad (76)$$

is chosen. As before, this choice is based upon the assumption that higher order terms are sufficiently small for $\varepsilon \searrow 0$ such that the order b in turn is large enough. To verify (75), we compute the stress tensor according to its definition (43). In the following, f -indices at physical moment expressions are omitted for the sake of simplicity. At first, we substitute the material derivative and use the mass conservation to obtain

$$\begin{aligned} \frac{D}{Dt} M_f^{\text{eq}} &= \left(\frac{1}{\rho} \frac{D}{Dt} \rho + 3\varepsilon^2 \varpi_\varepsilon \mathbf{c}_\varpi \cdot \frac{D}{Dt} \mathbf{u} - \frac{3\varepsilon^2 \mathbf{c}_\varpi \cdot \mathbf{F}}{m} \right) M_f^{\text{eq}} \\ &= \left[\frac{1}{\rho} (\partial_t + \mathbf{v} \cdot \nabla_{\mathbf{x}}) \rho + 3\varepsilon^2 \varpi_\varepsilon \mathbf{c}_\varpi \cdot (\partial_t + \mathbf{v} \cdot \nabla_{\mathbf{x}}) \mathbf{u} - \frac{3\varepsilon^2 \mathbf{c}_\varpi \cdot \mathbf{F}}{m} \right] M_f^{\text{eq}} \\ &= \left[\frac{1}{\rho} (-\mathbf{u} \cdot \nabla_{\mathbf{x}} \rho - \rho \nabla_{\mathbf{x}} \cdot \mathbf{u} + \mathbf{v} \cdot \nabla_{\mathbf{x}} \rho) + 3\varepsilon^2 \varpi_\varepsilon \mathbf{c}_\varpi \cdot (\partial_t + \mathbf{v} \cdot \nabla_{\mathbf{x}}) \mathbf{u} - \frac{3\varepsilon^2 \mathbf{c}_\varpi \cdot \mathbf{F}}{m} \right] M_f^{\text{eq}} \end{aligned}$$

$$= \left[- \underbrace{\nabla_{\mathbf{x}} \cdot \mathbf{u}}_{=: a_f} + \underbrace{\frac{\rho}{\rho} \cdot \nabla_{\mathbf{x}} \rho}_{=: b_f} + \underbrace{3\varepsilon^2 \varpi_\varepsilon \mathbf{c}_\varpi \cdot \partial_t \mathbf{u}}_{=: c_f} + \underbrace{3\varepsilon^2 \varpi_\varepsilon \mathbf{c}_\varpi \cdot (\mathbf{v} \cdot \nabla_{\mathbf{x}}) \mathbf{u}}_{=: d_f} - \underbrace{\frac{3\varepsilon^2 \mathbf{c}_\varpi \cdot \mathbf{F}}{m}}_{=: e_f} \right] M_f^{\text{eq}} \quad (77)$$

in \mathfrak{R} , where

$$\mathbf{c} := \mathbf{v} - \mathbf{u}, \quad (78)$$

$$\mathbf{c}_\varpi := \mathbf{v} - \varpi_\varepsilon \mathbf{u}, \quad (79)$$

are relative velocities, *i.e.* the deviation of the particle velocities \mathbf{v} from the local mean \mathbf{u} . Inserting the derivative (77) in (76) yields

$$f = M_f^{\text{eq}} [1 - 3\varepsilon^2 \nu (-a_f + b_f + c_f + d_f + e_f)] \quad \text{in } \mathfrak{R}. \quad (80)$$

Secondly, we evaluate the velocity space integrals of the individual terms a_f, b_f, \dots, e_f . To this end, we use the symmetric properties of M_f^{eq} and the fact that M_f^{eq}/n is a normal distribution with covariance matrix $1/(3\varepsilon^2) \mathbf{I}_d$. In Ω_T and for any $i, j, k, l \in \{1, 2, \dots, d\}$ we verify that

$$\begin{aligned} m \int_{\mathbb{R}^d} c_i c_j M_f^{\text{eq}} d\mathbf{v} &= m \int_{\mathbb{R}^d} c_{\varpi, i} c_{\varpi, j} M_f^{\text{eq}} d\mathbf{v} - m \int_{\mathbb{R}^d} (1 - \varpi_\varepsilon) u_i [2v_j - (1 + \varpi_\varepsilon) u_j] M_f^{\text{eq}} d\mathbf{v} \\ &= \frac{\rho}{3\varepsilon^2} \delta_{ij} - \rho (1 - \varpi_\varepsilon)^2 u_i u_j \\ &= p \delta_{ij} + \mathcal{O}(\varepsilon^4), \end{aligned} \quad (81)$$

as well as

$$\begin{aligned} m \int_{\mathbb{R}^d} c_i c_j c_k M_f^{\text{eq}} d\mathbf{v} &= m \underbrace{\int_{\mathbb{R}^d} c_{\varpi, i} c_{\varpi, j} c_{\varpi, k} M_f^{\text{eq}} d\mathbf{v}}_{=0} \\ &\quad + (\varpi_\varepsilon - 1) \rho u_i \left[\frac{1}{3\varepsilon^2} \delta_{jk} - (1 - \varpi_\varepsilon)^2 u_j u_k \right] \\ &\quad + (\varpi_\varepsilon - 1) \rho u_j \left[\frac{1}{3\varepsilon^2} \delta_{ik} - (1 - \varpi_\varepsilon)^2 u_i u_k \right] \\ &\quad + (\varpi_\varepsilon - 1) \rho u_k \left[\frac{1}{3\varepsilon^2} \delta_{ij} - (1 - \varpi_\varepsilon)^2 u_i u_j \right] \\ &= \sum_{\substack{\alpha\beta\gamma \in \\ \{ijk, jik, kij\}}} \left\{ (\varpi_\varepsilon - 1) \rho u_\alpha \left[\frac{1}{3\varepsilon^2} \delta_{\beta\gamma} - (1 - \varpi_\varepsilon)^2 u_\beta u_\gamma \right] \right\} \\ &= \mathcal{O}(1), \end{aligned} \quad (82)$$

and

$$\begin{aligned} m \int_{\mathbb{R}^d} c_i c_j c_{\varpi, k} v_l M_f^{\text{eq}} d\mathbf{v} &= \rho \left\{ \frac{1}{9\varepsilon^4} (\delta_{ij} \delta_{kl} + \delta_{ik} \delta_{jl} + \delta_{il} \delta_{jk}) \right. \\ &\quad + (\varpi_\varepsilon - 1)^2 u_i u_j \left[\frac{1}{3\varepsilon^2} \delta_{kl} - (1 - \varpi_\varepsilon)^2 u_k u_l \right] \\ &\quad + (\varpi_\varepsilon - 1) \varpi_\varepsilon u_i u_l \left[\frac{1}{3\varepsilon^2} \delta_{jk} - (1 - \varpi_\varepsilon)^2 u_j u_k \right] \\ &\quad \left. + (\varpi_\varepsilon - 1) \varpi_\varepsilon u_j u_l \left[\frac{1}{3\varepsilon^2} \delta_{ik} - (1 - \varpi_\varepsilon)^2 u_i u_k \right] \right\}, \end{aligned}$$

$$= \frac{\rho}{9\varepsilon^4}(\delta_{ij}\delta_{kl} + \delta_{ik}\delta_{jl} + \delta_{il}\delta_{jk}) + \mathcal{O}(1). \quad (83)$$

The order estimates hold since, by construction $\varpi_\varepsilon - 1 \in \mathcal{O}(\varepsilon^2)$. Hence, we obtain

$$\begin{aligned} m \int_{\mathbb{R}^d} c_i c_j a_f M_f^{\text{eq}} d\mathbf{v} &= \left(m \int_{\mathbb{R}^d} c_i c_j M_f^{\text{eq}} d\mathbf{v} \right) \partial_{x_k} u_k \\ &\stackrel{(81)}{=} \left(\frac{\rho}{3\varepsilon^2} + \mathcal{O}(\varepsilon^4) \right) \partial_{x_k} u_k \\ &= \frac{\rho}{3\varepsilon^2} \partial_{x_k} u_k + \mathcal{O}(\varepsilon^4), \end{aligned} \quad (84)$$

$$\begin{aligned} m \int_{\mathbb{R}^d} c_i c_j b_f M_f^{\text{eq}} d\mathbf{v} &= \left(m \int_{\mathbb{R}^d} c_i c_j c_k M_f^{\text{eq}} d\mathbf{v} \right) \frac{1}{\rho} \partial_{x_k} \rho \\ &\stackrel{(82)}{=} \mathcal{O}(1), \end{aligned} \quad (85)$$

$$\begin{aligned} m \int_{\mathbb{R}^d} c_i c_j c_f M_f^{\text{eq}} d\mathbf{v} &= \left(m \int_{\mathbb{R}^d} c_i c_j c_k M_f^{\text{eq}} d\mathbf{v} \right) 3\varepsilon^2 \varpi_\varepsilon \partial_t u_k \\ &\stackrel{(82)}{=} \mathcal{O}(\varepsilon^2), \end{aligned} \quad (86)$$

$$\begin{aligned} m \int_{\mathbb{R}^d} c_i c_j d_f M_f^{\text{eq}} d\mathbf{v} &= \left(m \int_{\mathbb{R}^d} c_i c_j c_{\varpi, k} v_l M_f^{\text{eq}} d\mathbf{v} \right) 3\varepsilon^2 \varpi_\varepsilon \partial_{x_l} u_k \\ &\stackrel{(83)}{=} 3\varepsilon^2 \varpi_\varepsilon \partial_{x_l} u_k \left[\frac{\rho}{9\varepsilon^4} (\delta_{ij}\delta_{kl} + \delta_{ik}\delta_{jl} + \delta_{il}\delta_{jk}) + \mathcal{O}(1) \right] \\ &\stackrel{(68)}{=} \partial_{x_l} u_k \frac{\rho}{3\varepsilon^2} (\delta_{ij}\delta_{kl} + \delta_{ik}\delta_{jl} + \delta_{il}\delta_{jk}) + \mathcal{O}(1), \end{aligned} \quad (87)$$

$$\begin{aligned} m \int_{\mathbb{R}^d} c_i c_j e_f M_f^{\text{eq}} d\mathbf{v} &= \rho(\varpi_\varepsilon - 1) F_k u_j \delta_{ik} \\ &= \mathcal{O}(\varepsilon^2). \end{aligned} \quad (88)$$

Third and finally, each \mathbf{P} -component P_{ij} for $i, j \in \{1, 2, \dots, d\}$ is computable in \mathfrak{R} . Via reordering terms, we obtain

$$\begin{aligned} P_{ij} &= m \int_{\mathbb{R}^d} c_i c_j [1 - 3\nu\varepsilon^2(-a_f + b_f + c_f + d_f + e_f)] M_f^{\text{eq}} d\mathbf{v} \\ &= p\delta_{ij} - 3\nu\varepsilon^2 \left[-\frac{\rho}{3\varepsilon^2} \partial_{x_k} u_k + \partial_{x_l} u_k \frac{\rho}{3\varepsilon^2} (\delta_{ij}\delta_{kl} + \delta_{ik}\delta_{jl} + \delta_{il}\delta_{jk}) + \mathcal{O}(1) \right] \\ &= p\delta_{ij} + \nu\rho [\delta_{ij}\partial_{x_k} u_k - \partial_{x_l} u_k (\delta_{ij}\delta_{kl} + \delta_{ik}\delta_{jl} + \delta_{il}\delta_{jk})] + \mathcal{O}(\varepsilon^2) \\ &= p\delta_{ij} - \nu\rho (\partial_{x_i} u_j + \partial_{x_j} u_i) + \mathcal{O}(\varepsilon^2) \end{aligned} \quad (89)$$

and thus equivalently

$$\mathbf{P} = p\mathbf{I}_d - 2\nu\rho\mathbf{D} + \mathcal{O}(\varepsilon^2) \quad \text{in } \Omega_T, \quad (90)$$

which formally proves the approximate recovery of the HNSE (35) in the hydrodynamic limit.

To summarize the contribution of Section 3, we state the following main results.

Theorem 3.15. *Let $\varepsilon > 0$ and f^* denote a solution of the ε -parametrized homogenized BGK Boltzmann equation (69). In the diffusive limit ($Kn \searrow 0$ and $Ma \searrow 0$ with constant Re), the velocity moment \mathbf{u}_{f^*} (41) satisfies the HNSE (35) up to the order $\mathcal{O}(\varepsilon^2)$.*

Proof. As carried out above, deriving the velocity moment equation (59) in Step 1 and computing the pressure tensor approximation (90) in Step 3 by using the power series expansion (74) from Step 2 complete the proof. \square

Remark 3.16. The diffusive limit in Theorem 3.15 forms the basis for the limit consistent discretization in the sequel (part II [64]). As illustrated in Figure 1, a discretization of velocity and space-time with mapping of the grid parameters to a function of ε will lead to a homogenized lattice Boltzmann equation that approximates solutions to the HNSE (35) as moments of f .

4. CONCLUSION

The overall aim of this series of works is to construct HLBM that approximate the governing equations for homogenized nonstationary nonlinear fluid flow through porous media.

Summarizing the present work (part I), we make two contributions. At first, we recall the existing framework of Allaire for homogenizing the NSE with specific geometric configurations. We gather proven results towards a unified homogenization of incompressible nonstationary NSE in the framework of porous media as abstracted periodically arranged obstacles. We restate the stationary simplification and subsequently include time-dependency. In the latter case, we form Conjecture 2.10 that consists of four cases as the result of homogenization depending on the size of the obstacles: (i) nonstationary NSE, (ii) nonstationary Brinkman law, (iii) time-dependent Darcy’s law, and (iv) Darcy’s law with memory. We isolate the missing proofs and review existing results. In addition, an application-oriented rationale is presented that determines the porosity range that is recoverable by the mathematical model. Based on that, we formulate a modified nonstationary Brinkman law which is termed HNSE (35) and serves as a unified targeted PDE system for the HLBM to be proposed in the sequel (part II [64]). Second, as a first step toward the HLBM, we propose a kinetic model, the homogenized BGK Boltzmann equation (58), which approximates the non-stationary HNSE (35) in a diffusive scaling limit. We formally prove that the zeroth and first order moments of the kinetic model provide solutions to the mass and momentum balance variables of the macroscopic model up to certain orders in the scaling parameter. Specifically, the stress tensor is approximated with $O(\varepsilon^2)$ in the diffusive limit.

Future studies with respect to mathematical and kinetic model extensions should involve mixed boundary conditions at the porous matrix [18], porous–void interface conditions [26], porosity gradients in the solid matrix [15] or investigating modeling possibilities of anisotropic permeability tensors [10, 55].

In the sequel of this work (part II [64]), we construct and validate HLBM to approximate the HNSE (35) for porous media flow (see Fig. 1) within the limit consistency framework introduced in [58]. Therein, the limit consistency at most of the order of two of the moments of a solution to the homogenized lattice Boltzmann equation toward the pressure and velocity, respectively, of the HNSE (35) is formally proven. The derivation is based on determining the truncation errors of the governing families of equations at each discretization level of the homogenized BGK Boltzmann equation (58). In addition, HLBM simulations in various parameter regimes are conducted, numerically validating the present theoretical predictions.

FUNDING

This work was supported by the Deutsche Forschungsgemeinschaft (DFG, German Research Foundation, DOI: [10.13039/501100001659](https://doi.org/10.13039/501100001659)), project number [382064892/SPP2045](https://www.dfg.de/en/DFG-Grants/DFG-Grants-Details/382064892/SPP2045) as well as project number [468824876](https://www.dfg.de/en/DFG-Grants/DFG-Grants-Details/468824876). S. Simonis sincerely thanks Fabian Klemens and Eduard Feireisl for valuable discussions.

DATA AVAILABILITY STATEMENT

The research data associated with this article are included in the article.

AUTHOR CONTRIBUTION STATEMENT

S. Simonis: Conceptualization, Methodology, Validation, Formal analysis, Investigation, Writing – Original Draft, Writing – Review & Editing, Visualization, Supervision, Project administration; **N. Hafen:** Methodology, Validation, Investigation, Writing – Review & Editing, Funding acquisition; **J. Jeßberger:** Writing – Review & Editing, Methodology, Formal analysis; **D. Dapelo:** Writing – Review & Editing; **G. Thäter:** Writing – Review & Editing, Supervision; **M.J. Krause:** Resources, Writing – Review & Editing, Supervision, Funding acquisition. All authors read and approved the final version of the manuscript.

REFERENCES

- [1] G. Allaire, *Homogénéisation des équations de Stokes et de Navier–Stokes*. Ph.D. thesis, Centre d’Etudes Nucléaires de Saclay (1990). http://inis.iaea.org/search/search.aspx?orig_q=RN:22020229. CEA-N–2638.
- [2] G. Allaire, Continuity of the Darcy’s law in the low-volume fraction limit. *Annali della Scuola Normale Superiore di Pisa – Classe di Scienze* **18** (1991) 475–499. http://www.numdam.org/item/ASNSP_1991_4_18_4_475_0.
- [3] G. Allaire, Homogenization of the Navier–Stokes equations in open sets perforated with tiny holes I: abstract framework, a volume distribution of holes. *Arch. Ration. Mech. Anal.* **113** (1991) 209–259.
- [4] G. Allaire, Homogenization of the Navier–Stokes equations in open sets perforated with tiny holes II: non-critical sizes of the holes for a volume distribution and a surface distribution of holes. *Arch. Ration. Mech. Anal.* **113** (1991) 261–298.
- [5] G. Allaire, Homogenization of the Navier–Stokes equations and derivation of Brinkman’s law, in *Mathématiques appliquées aux sciences de l’ingénieur: 2e colloque franco-chilien de mathématiques appliquées* (Santiago, 1989), edited by C. Carasso, C. Conca, J.-P. Puel and R. Correa. Cépaduès (1991) 7–20.
- [6] G. Allaire, Homogenization of the unsteady Stokes equations in porous media, in *Progress in Partial Differential Equations: Calculus of Variations, Applications*. *Pitman Research Notes in Mathematics Series*, edited by C. Bandle, J. Bemelmans, M. Chipot, M. Grüter and J. Saint Jean Paulin. Vol. 267. Longman Scientific & Technical (1992) 109.
- [7] G. Allaire, Homogenization and two-scale convergence. *SIAM J. Math. Anal.* **23** (1992) 1482–1518.
- [8] G. Allaire, CEA-EDF-INRIA school on homogenization, December 13–16, Lecture 2 (2010). <http://www.cmap.polytechnique.fr/~allaire/homog/>.
- [9] H. Babovsky, *Die Boltzmann-Gleichung: Modellbildung-Numerik-Anwendungen*. Springer/Vieweg+Teubner (1998).
- [10] B. Bang and D. Lukkassen, Application of homogenization theory related to Stokes flow in porous media. *App. Math.* **44** (1999) 309–319.
- [11] J. Bear, *Dynamics of Fluids in Porous Media*. American Elsevier Publishing Co (1972).
- [12] P.L. Bhatnagar, E.P. Gross and M. Krook, A model for collision processes in gases. I. Small amplitude processes in charged and neutral one-component systems. *Phys. Rev.* **94** (1954) 511–525.
- [13] H. Brinkman, On the permeability of media consisting of closely packed porous particles. *Flow Turbul. Combust.* **1** (1949) 81.
- [14] F. Bukreev, S. Simonis, A. Kummerländer, J. Jessberger and M.J. Krause, Consistent lattice Boltzmann methods for the volume averaged Navier–Stokes equations. *J. Comput. Phys.* **490** (2023) 112301.
- [15] M.P. Dalwadi, I.M. Griffiths and M. Bruna, Understanding how porosity gradients can make a better filter using homogenization theory. *Proc. R. Soc. A* **471** (2015) 20150464.
- [16] D. Dapelo, S. Simonis, M.J. Krause and J. Bridgeman, Lattice–Boltzmann coupled models for advection–diffusion flow on a wide range of Péclet numbers. *J. Comput. Sci.* **51** (2021) 101363.
- [17] H.P.G. Darcy, *Les Fontaines publiques de la ville de Dijon*. Exposition et application des principes à suivre et des formules à employer dans les questions de distribution d’eau, etc. V. Dalmont (1856).
- [18] J. Fabricius, E. Miroshnikova and P. Wall, Homogenization of the Stokes equation with mixed boundary condition in a porous medium. *Cogent Math.* **4** (2017) 1327502.
- [19] E. Feireisl, A. Novotný and T. Takahashi, Homogenization and singular limits for the complete Navier–Stokes–Fourier system. *J. Pure Appl. Math.* **94** (2010) 33–57.
- [20] E. Feireisl, Y. Namlyeyeva and Š. Nečasová, Homogenization of the evolutionary Navier–Stokes system. *Math. Manuscripts* **149** (2016) 251–274.
- [21] F. Feppon, High order homogenization of the Stokes system in a periodic porous medium. *SIAM J. Math. Anal.* **53** (2021) 2890–2924.
- [22] F. Feppon and W. Jing, High order homogenized Stokes models capture all three regimes. *SIAM J. Math. Anal.* **54** (2022) 5013–5040.
- [23] P. Forchheimer, Wasserbewegung durch Boden. *Zeitschrift des Vereins deutscher Ingenieure* **45** (1901) 1782–1788.
- [24] T.A. Ghezzehei and D. Or, Pore-space dynamics in a soil aggregate bed under a static external load. *Soil Sci. Soc. Am. J.* **67** (2003) 12–19.
- [25] A.N. Gorban, Hilbert’s sixth problem: the endless road to rigour. *Philos. Trans. R. Soc. A* **376** (2018) 20170238.
- [26] M. Griebel and M. Klitz, Homogenisation and numerical simulation of flow in geometries with textile microstructures. *SIAM Multiscale Model. Simul.* **8** (2010) 1439–1460.

- [27] Z. Guo and T. Zhao, Lattice Boltzmann model for incompressible flows through porous media. *Phys. Rev. E* **66** (2002) 036304.
- [28] Z. Guo, J. Li and K. Xu, Unified preserving properties of kinetic schemes. *Phys. Rev. E* **107** (2023) 025301.
- [29] M. Haussmann, S. Simonis, H. Nirschl and M.J. Krause, Direct numerical simulation of decaying homogeneous isotropic turbulence – numerical experiments on stability, consistency and accuracy of distinct lattice Boltzmann methods. *Int. J. Modern Phys. C* **30** (2019) 1–29.
- [30] M. Haussmann, P. Reinshaus, S. Simonis, H. Nirschl and M.J. Krause, Fluid–structure interaction simulation of a coriolis mass flowmeter using a lattice Boltzmann method. *Fluids* **6** (2021) 167.
- [31] X. He and L.-S. Luo, Theory of the lattice Boltzmann method: from the Boltzmann equation to the lattice Boltzmann equation. *Phys. Rev. E* **56** (1997) 6811–6817.
- [32] U. Hornung, Homogenization and Porous Media. Vol. 6. Springer, New York (1997).
- [33] M. Junk, A. Klar and L.-S. Luo, Asymptotic analysis of the lattice Boltzmann equation. *J. Comput. Phys.* **210** (2005) 676–704.
- [34] M. Klitz, *Homogenised fluid flow equations in porous media with application to permeability computations in textiles*. Diploma thesis, Institut für Numerische Simulation, Universität Bonn (2006). http://wissrech.ins.uni-bonn.de/teaching/diplom/diplom_klitz.pdf.
- [35] M.J. Krause, *Fluid flow simulation and optimisation with lattice Boltzmann methods on high performance computers: application to the human respiratory system*. Doctoral thesis, Karlsruhe Institute of Technology (KIT) (2010). <https://publikationen.bibliothek.kit.edu/1000019768>.
- [36] M.J. Krause, G. Thäter and V. Heuveline, Adjoint-based fluid flow control and optimisation with lattice Boltzmann methods. *Comput. Math. App.* **65** (2013) 945–960.
- [37] M.J. Krause, A. Kummerländer, S.J. Avis, H. Kusumaatmaja, D. Dapelo, F. Klemens, M. Gaedtke, N. Hafen, A. Mink, R. Trunk, J.E. Marquardt, M.-L. Maier, M. Haussmann and S. Simonis, OpenLB – Open source lattice Boltzmann code. *Comput. Math. App.* **81** (2021) 258–288.
- [38] A. Kummerländer, M. Dorn, M. Frank and M.J. Krause, Implicit propagation of directly addressed grids in lattice Boltzmann methods. *Concurrency Comput. Pract. Exp.* **35** (2022) e7509.
- [39] A. Kummerländer, F. Bukreev, S.F.R. Berg, M. Dorn and M.J. Krause, Advances in computational process engineering using lattice Boltzmann methods on high performance computers, in High Performance Computing in Science and Engineering’22, edited by W.E. Nagel, D.H. Kröner and M.M. Resch. Springer Nature Switzerland, Cham (2024) 233–247.
- [40] P. Lallemand and L.-S. Luo, Theory of the lattice Boltzmann method: dispersion, dissipation, isotropy, Galilean invariance, and stability. *Phys. Rev. E* **61** (2000) 6546.
- [41] P. Lallemand, L.-S. Luo, M. Krafczyk and W.-A. Yong, The lattice Boltzmann method for nearly incompressible flows. *J. Comput. Phys.* **431** (2021) 109713.
- [42] V. Laptev, *Numerical solution of coupled flow in plain and porous media*. Doctoral thesis, Technische Universität Kaiserslautern, 2003. <http://nbn-resolving.de/urn:nbn:de:hbz:386-kluedo-17312>.
- [43] J. Leray, Sur le mouvement d’un liquide visqueux emplissant l’espace. *Acta Math.* **63** (1934) 193–248.
- [44] A. Mikelić, Homogenization of nonstationary Navier–Stokes equations in a domain with a grained boundary. *Annali di Matematica Pura ed Applicata* **158** (1991) 167–179.
- [45] A. Mikelić, Mathematical derivation of the Darcy-type law with memory effects, governing transient flow through porous medium. *Glasnik Matematički* **29** (1994) 57–77.
- [46] A. Mink, K. Schediwy, C. Posten, H. Nirschl, S. Simonis and M.J. Krause, Comprehensive computational model for coupled fluid flow, mass transfer, and light supply in tubular photobioreactors equipped with glass sponges. *Energies* **15** (2022) 7671.
- [47] S. Mischler, Uniqueness for the BGK-equation in \mathbb{R}^N and rate of convergence for a semi-discrete scheme. *Differ. Integral Equ.* **9** (1996) 1119–1138.
- [48] D. Nield, Convection in Porous Media, 5th edition. Springer, New York (2017).
- [49] P. Nithiarasu, K. Seetharamu and T. Sundararajan, Natural convective heat transfer in a fluid saturated variable porosity medium. *Int. J. Heat Mass Trans.* **40** (1997) 3955–3967.
- [50] R.K. Padhy, A. Chandrasekhar and K. Suresh, FluTO: graded multi-scale topology optimization of large contact area fluid-flow devices using neural networks. *Eng. Comput.* **40** (2024) 971–987.
- [51] B. Perthame, Global existence to the BGK model of Boltzmann equation. *J. Differ. Equ.* **82** (1989) 191–205.
- [52] B. Perthame and M. Pulvirenti, Weighted L^∞ bounds and uniqueness for the Boltzmann BGK model. *Arch. Ration. Mech. Anal.* **125** (1993) 289–295.

- [53] F. Rao and Y. Jin, Possibility for survival of macroscopic turbulence in porous media with high porosity. *J. Fluid Mech.* **937** (2022) A17.
- [54] L. Saint-Raymond, From the BGK model to the Navier–Stokes equations. *Annales Scientifiques de l'École Normale Supérieure* **36** (2003) 271–317.
- [55] T. Seta, Lattice Boltzmann method for fluid flows in anisotropic porous media with Brinkman equation. *J. Fluid Sci. Technol.* **4** (2009) 116–127.
- [56] S. Simonis, *Lattice Boltzmann methods for partial differential equations*. Doctoral thesis, Karlsruhe Institute of Technology (KIT) (2023). <https://publikationen.bibliothek.kit.edu/1000161726>.
- [57] S. Simonis and M.J. Krause, Forschungsnahe Lehre unter Pandemiebedingungen. *Mitteilungen der Deutschen Mathematiker-Vereinigung* **30** (2022) 43–45.
- [58] S. Simonis and M.J. Krause, Limit consistency of lattice Boltzmann equations. Preprint [arXiv:2208.06867](https://arxiv.org/abs/2208.06867) (2022).
- [59] S. Simonis and S. Mishra, Computing statistical Navier–Stokes solutions, in *Hyperbolic Balance Laws: Interplay between Scales and Randomness*, edited by R. Abgrall, M. Garavello, M. Lukáčová-Medvid'ová and K. Trivisa. Number 1 in Oberwolfach Report 21. EMS Press (2024) 567–656.
- [60] S. Simonis, M. Frank and M.J. Krause, On relaxation systems and their relation to discrete velocity Boltzmann models for scalar advection–diffusion equations. *Philos. Trans. R. Soc. A* **378** (2020) 20190400.
- [61] S. Simonis, M. Haussmann, L. Kronberg, W. Dörfler and M.J. Krause, Linear and brute force stability of orthogonal moment multiple-relaxation-time lattice Boltzmann methods applied to homogeneous isotropic turbulence. *Philos. Trans. R. Soc. A* **379** (2021) 20200405.
- [62] S. Simonis, D. Oberle, M. Gaedtke, P. Jenny and M.J. Krause, Temporal large eddy simulation with lattice Boltzmann methods. *J. Comput. Phys.* **454** (2022) 110991.
- [63] S. Simonis, M. Frank and M.J. Krause, Constructing relaxation systems for lattice Boltzmann methods. *Appl. Math. Lett.* **137** (2023) 108484.
- [64] S. Simonis, K. Dominic, A. Kummerländer, N. Hafen, S. Ito, D. Dapelo, G. Thäter and M.J. Krause, Homogenized lattice Boltzmann methods for fluid flow through porous media - part II: discretization and numerical experiments. To appear (2025).
- [65] S. Simonis, J. Nguyen, S.J. Avis, W. Dörfler and M.J. Krause, Binary fluid flow simulations with free energy lattice Boltzmann methods. *Discrete Continuous Dyn. Syst. – S* **17** (2024) 3278–3294.
- [66] M. Siodlaczek, M. Gaedtke, S. Simonis, M. Schweiker, N. Homma and M.J. Krause, Numerical evaluation of thermal comfort using a large eddy lattice Boltzmann method. *Building Environ.* **192** (2021) 107618.
- [67] M.A. Spaid and F.R. Phelan Jr., Lattice Boltzmann methods for modeling microscale flow in fibrous porous media. *Phys. Fluids* **9** (1997) 2468–2474.
- [68] Y. Tanabe, K. Yaji and K. Ushijima, Topology optimization using the lattice Boltzmann method for unsteady natural convection problems. *Struct. Multidiscipl. Optim.* **66** (2023) 103.
- [69] M. Zhong, T. Xiao, M.J. Krause, M. Frank and S. Simonis, A stochastic Galerkin lattice Boltzmann method for incompressible fluid flows with uncertainties. *J. Comput. Phys.* **517** (2024) 113344.

Please help to maintain this journal in open access!



This journal is currently published in open access under the Subscribe to Open model (S2O). We are thankful to our subscribers and supporters for making it possible to publish this journal in open access in the current year, free of charge for authors and readers.

Check with your library that it subscribes to the journal, or consider making a personal donation to the S2O programme by contacting subscribers@edpsciences.org.

More information, including a list of supporters and financial transparency reports, is available at <https://edpsciences.org/en/subscribe-to-open-s2o>.